Search for pair production of first generation scalar Leptoquarks at CMS

[1]M.A. Bhat, [1]G.B. Mohanty, [1]T. Aziz, [1]B. Mahakud
[2]S.I. Cooper, [2]P. Rumerio

[1]Tata Institute of Fundamental Research (India)
[2]University of Alabama (USA)

March 19, 2018
DHEP Seminar

Introduction

- Leptoquarks (LQs) arise in many theories beyond the standard model such as Pati-Salam, GUTs, technicolor etc.
- They appear as spin-0 or spin-1 bosons carrying both baryon and lepton numbers as well as fractional electric charge

- We are looking for pair production of 1st generation scalar LQs, produced mainly via gluon-gluon fusion at the LHC

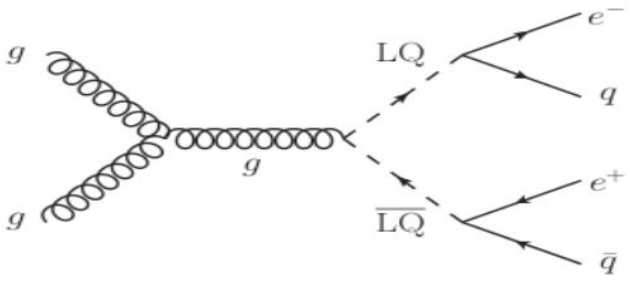

(1) $eejj$ channel

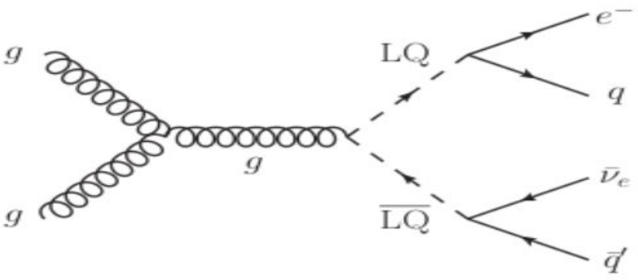

(2) $e\nu jj$ channel

Analysis Overview

- Signal final state comprises at least two high-p_T electrons and two high-p_T jets for the *eejj* channel and an electron, MET and two high-p_T jets for the *evjj* channel
- Define a selection dominated by background ("preselection") used for data-MC background comparison
- Optimise final selections as a function of LQ mass

- Final selection variables:

eejj channel:

S_T $= p_T^{e1} + p_T^{e2} + p_T^{jet1} + p_T^{jet2}$

M_{min}^{ej} : LQ candidates are reconstructed using the e-j pairing with minimum $|M_{LQ1} - M_{LQ2}|$

M_{ee}: Invariant mass of the di-electron system

evjj channel

S_T $= p_T^{e1} + MET + p_T^{jet1} + p_T^{jet2}$

M_{ej} : LQ candidates are reconstructed using the l-j pairing with minimum $|MT_{LQ1} - MT_{LQ2}|$

$m_T(e,v)$ *:* electron - neutrino transverse mass

MET: Missing transverse energy

Backgrounds

- ***Z+jets*** → dominant background in *eejj* channel but small contribution in *evjj* channel
- ***ttbar*** → significant contribution in both the channels
- ***QCD multijet*** → minor contribution in *eejj* channel but significant contribution in *evjj* channel
- ***W+jets*** → major background in *evjj* channel but minor contribution in *eejj* channel
- Other minor backgrounds in both the channels include:
    - *Diboson*
    - *Single top*
    - *Gamma + jets*

Preselection

Preselection *eejj*	
Variable	Cut
At least two electrons passing HEEP ID	p_T > 50 GeV, |η| < 2.5
>= 2 jets	p_T > 50 GeV, |η| < 2.4
M_{ee}	> 50 GeV
$p_T(ee)$	> 70 GeV
S_T	> 300 GeV

Preselection *eνjj*	
Variable	Cut
Exactly one electron passing HEEP ID	p_T > 50 GeV, |η| < 2.2
>= 2 jets	p_T > 50 GeV, |η| < 2.4
$m_T(e,\nu)$	> 50 GeV
$p_T(e,MET)$	> 70 GeV
S_T	> 300 GeV
MET	> 100 GeV
$\|\Delta\phi(MET,e)\|$	> 0.5
$\|\Delta\phi(MET,j1)\|$	> 0.5

Common selections

- No muons with p_T > 35 GeV, |η| < 2.4 and passing high p_T muon ID
- Jets: ak4PFCHS, loose ID
- MET: PFMET Type1XY
- Trigger: HLT_Ele27_WPTight_Gsf_v **OR** HLT_Ele115_CaloIdVT_GsfTrkIdT_v **OR** HLT_Photon175_v

Trigger Efficiency

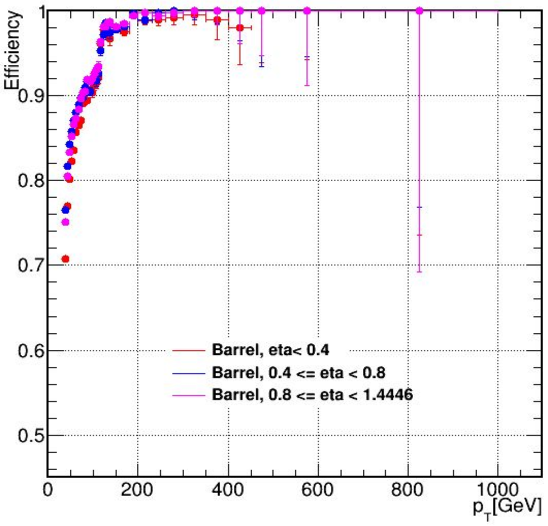

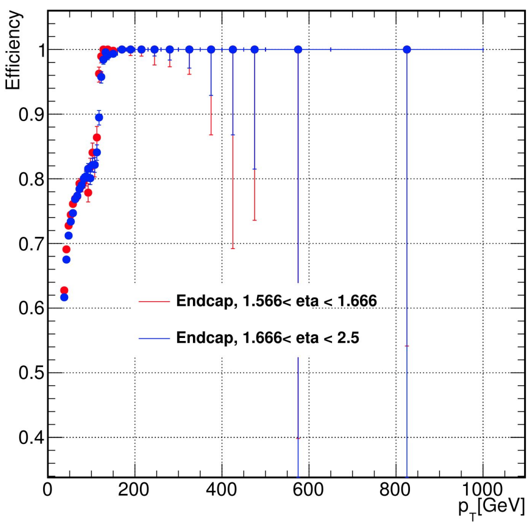

- *Results reviewed and approved by Egamma POG*

- Trigger efficiency is measured using the ‘tag and probe’ method exploiting the $Z(\rightarrow e^+e^-)$ decay
- Select events with two electrons having $60 < M_{ee} < 120$ GeV
- Require one electron to be the tag and the other be the probe
- Measure efficiency by calculating how many times the probe passes the trigger
- No trigger requirement is applied to the MC samples; rather the efficiency curve is applied

Backgrounds for *eejj*

DY+jets background:

- Shape from MC, normalise at preselection requiring $80 < M_{ee} < 100$ GeV
- Subtract other backgrounds using MC and QCD (data driven)
- Scale factor = 0.97 +/- 0.01(stat.)

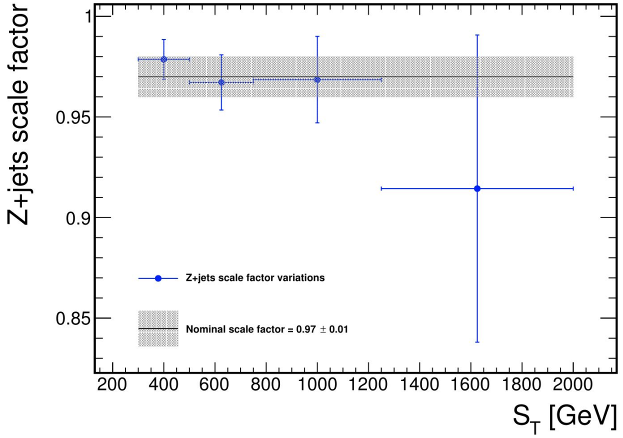

Variation of scale factor vs. S_T is flat

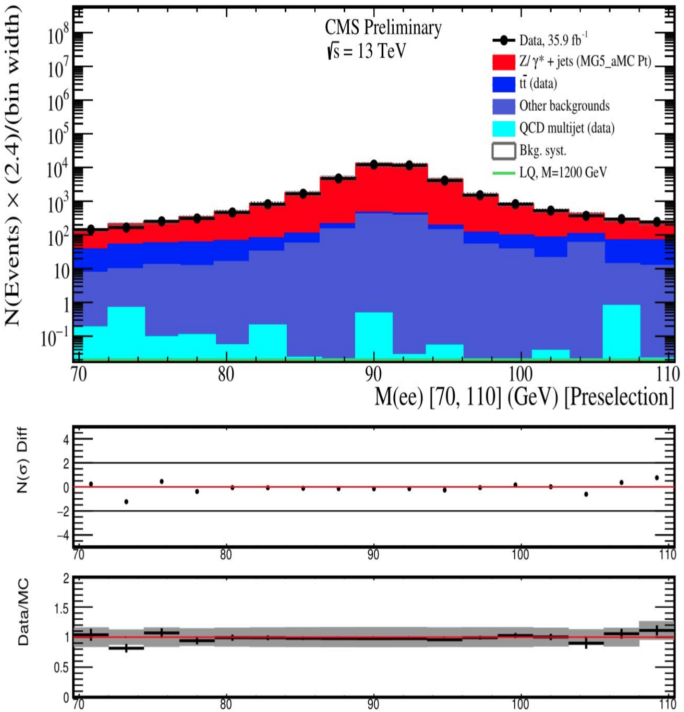

Backgrounds for *eejj*

ttbar background:

- Data driven prediction using *eμjj* events
- Formula used:

$$N^{ee}_{t\bar{t}} = N^{e\mu}_{t\bar{t}} \times R_{trigger} \times R_{ee,e\mu}$$

$$N^{e\mu}_{t\bar{t}} = N^{e\mu}_{Data} - N^{e\mu}_{OtherBkg'}$$

- Apply trigger efficiency only to the lead electron
- $R_{trigger}$ = 2-ε
- $R_{ee,e\mu}$ is obtained from ttbar MC
- $R_{ee,e\mu}$ = 0.479 +/- 0.003

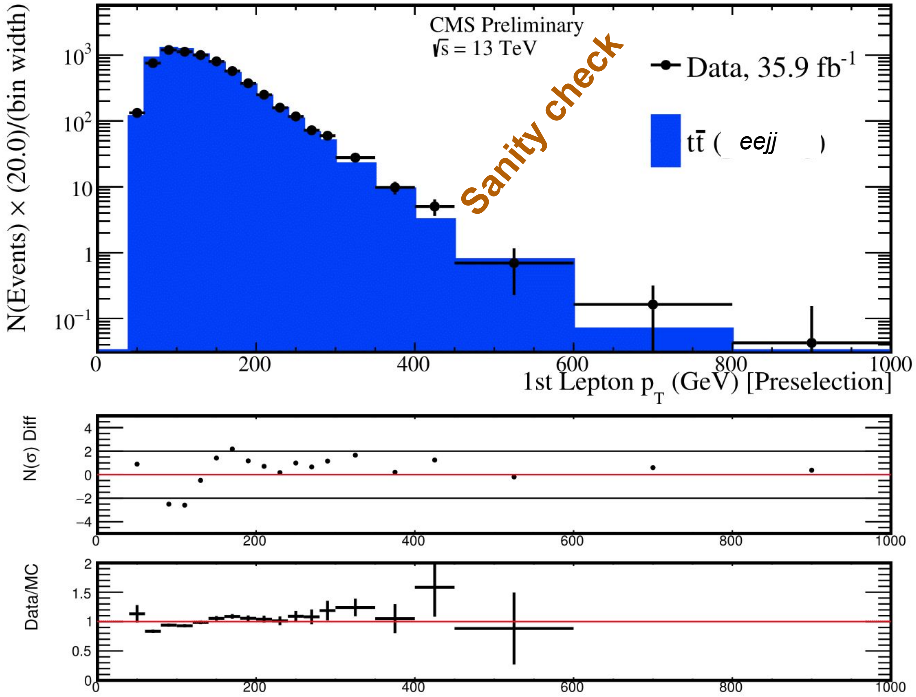

QCD Background

Use the fake rate method to estimate the QCD background

- Similar to as done in Z' analysis
- Measure:

$$\text{Fake rate} = \frac{N_{jets,sig}}{N_{e,loose}}$$

- To get the fake-rate an event is required to satisfy the following conditions:
    - Exactly one loose electron
    - Pass the single photon trigger, matching the loose electron* to the trigger object
- Measure the fake-rate in bins of η (barrel/2 endcap bins) and E_T for different jet multiplicities
- Used template method to get the fake-rate

Variable	Barrel Threshold	Endcap Threshold
* isEcalDriven	yes	yes
$\sigma_{i\eta i\eta}^{5\times5}$	<0.013	<0.034
$\lvert d_{xy}\rvert$ [cm]	<0.02	<0.05
H/E	<0.15	<0.10
Missing hits	<= 1	<= 1

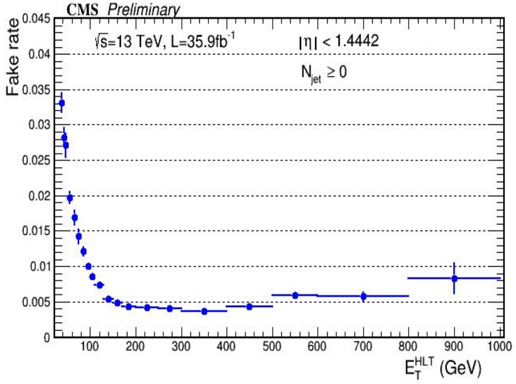

QCD Background

- Use track isolation as a template variable
- Define the signal region and sideband in the template variable
  - Signal region (SR): track isolation < 5 GeV (HEEP threshold)
  - Sideband (SB): 10 < track isolation< 20 GeV

- Use the ratio of the jet events in the SR compared to the SB to calculate the fake contribution in the SR

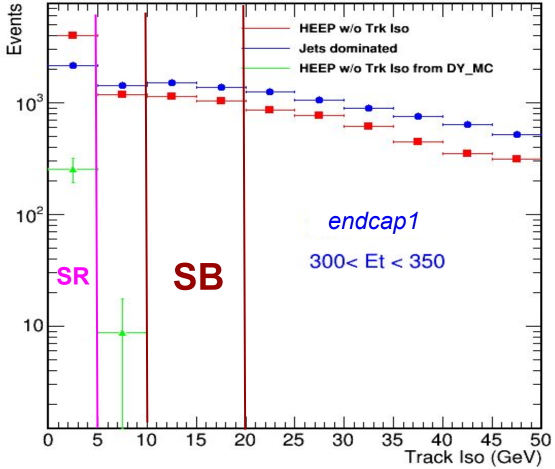

$$N_{jets,sig} = R^{\text{jets}}_{\text{SR/SB}} \times N_{\text{HEEP}'}(\text{SB})$$

Event yield:

$$N^{\text{QCD}}_{eejj} = \sum_{\text{loose eejj events}} \frac{P(e_{1,\text{tight}}|e_{1,\text{loose}} : p_T, \eta)}{1 - P(e_{1,\text{tight}}|e_{1,\text{loose}} : p_T, \eta)} \cdot \frac{P(e_{2,\text{tight}}|e_{2,\text{loose}} : p_T, \eta)}{1 - P(e_{2,\text{tight}}|e_{2,\text{loose}} : p_T, \eta)}$$

$$N^{\text{QCD}}_{e\nu jj} = \sum_{\text{loose e}\nu\text{jj events}} \frac{P(e_{\text{tight}}|e_{\text{loose}} : p_T, \eta)}{1 - P(e_{\text{tight}}|e_{\text{loose}} : p_T, \eta)}$$

Closure Test

- Prediction: Events with both electrons failing HEEP:

$$N^{QCD,exp}_{\text{loose } e,\text{tight } e} = \sum_{\text{loose } e,\text{loose } e} \frac{P(e_1)}{1-P(e_1)} + \frac{P(e_2)}{1-P(e_2)}$$

- Actual: Require exactly 1 electron passing HEEP in data; subtract non-QCD processes using MC
- In both cases *MET* < 100 GeV, S_T > 200 GeV, M_{ee} > 110 GeV

$$N^{QCD,exp}_{\text{loose } e,\text{tight } e} = 24237 \pm 922$$
$$N^{QCD,obs}_{\text{loose } e,\text{tight } e} = 26887 \pm 5252$$

In region with tighter S_T (340 GeV)

$$N^{QCD,exp}_{\text{loose } e,\text{tight } e} = 8416 \pm 323$$
$$N^{QCD,obs}_{\text{loose } e,\text{tight } e} = 7597 \pm 1279$$

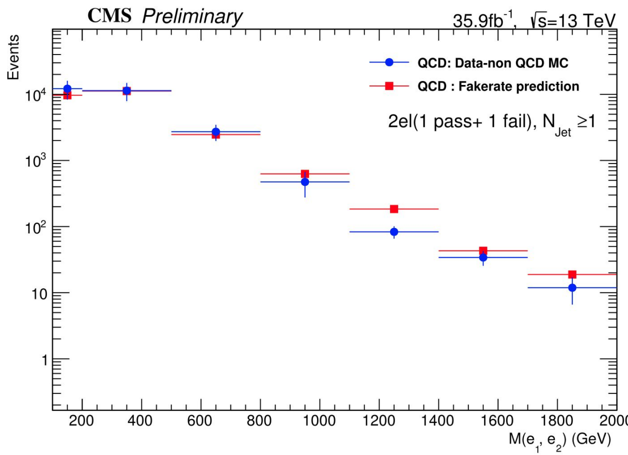

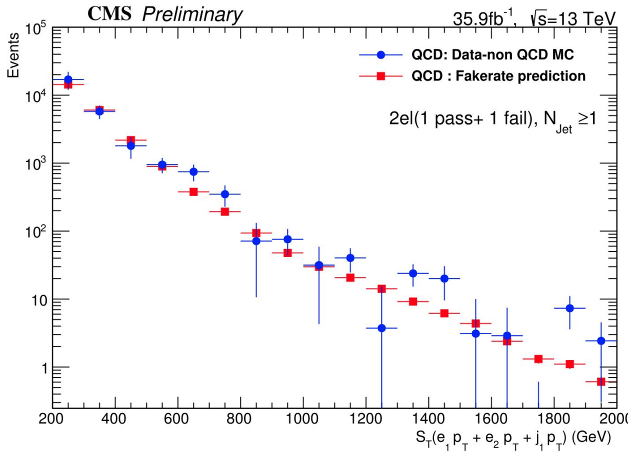

Preselection Distributions *eejj*

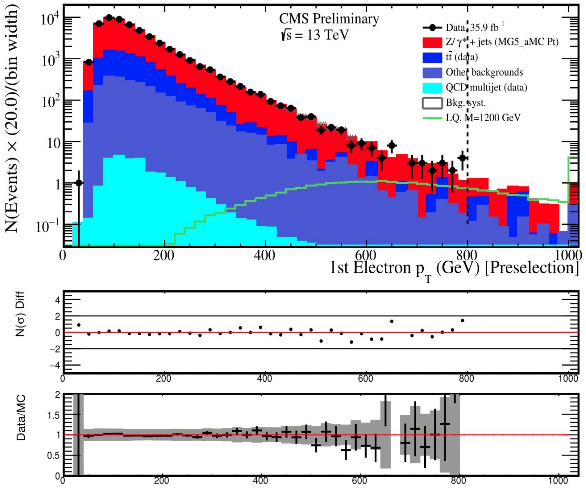

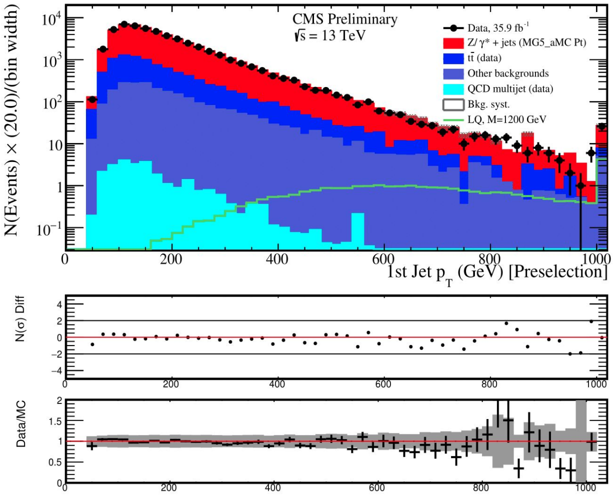

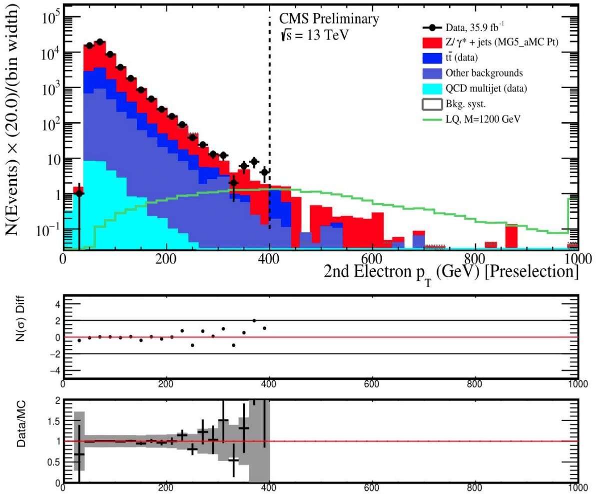

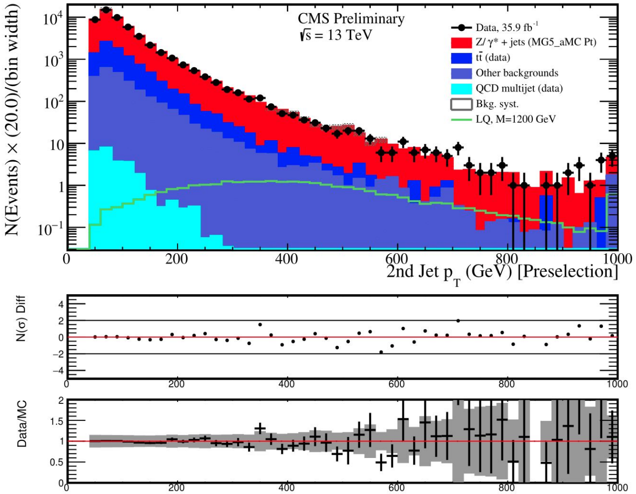

Kinematics of electrons and jets look well-modeled

Preselection Distributions *eejj*

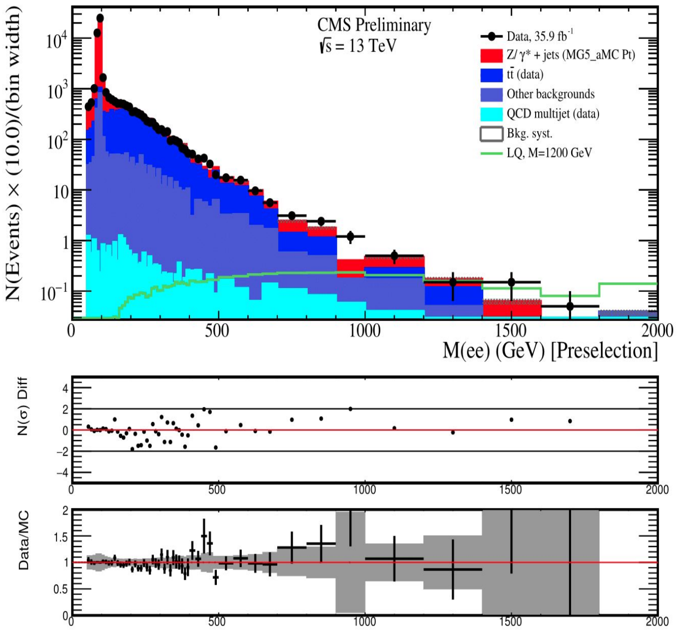

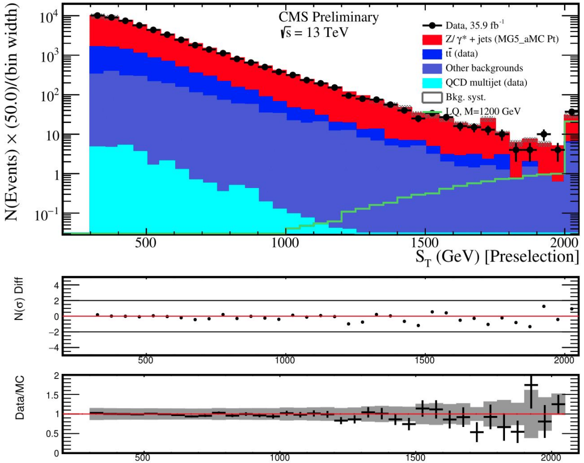

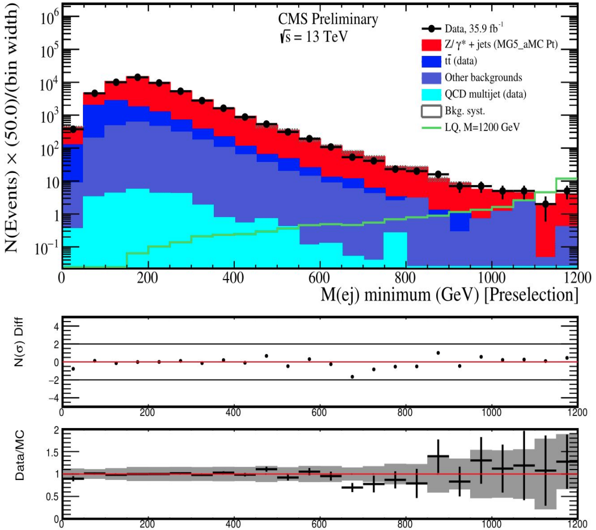

- *Selection variables also look good*

Backgrounds for *evjj*

W+jets and ttbar background:

- Shape from MC, normalised to data
- Define two control regions, one which enriches the sample with W+jets, and one which increases the ttbar contribution

W+jets control region

- *evjj preselection*
- *50 < $m_T(e,\nu)$ < 110 GeV*
- *Zero b-tagged jets*

ttbar control region

- *evjj preselection*
- *50 < $m_T(e,\nu)$ < 110 GeV*
- *At least 1 b-tagged jet*

W+jet control region

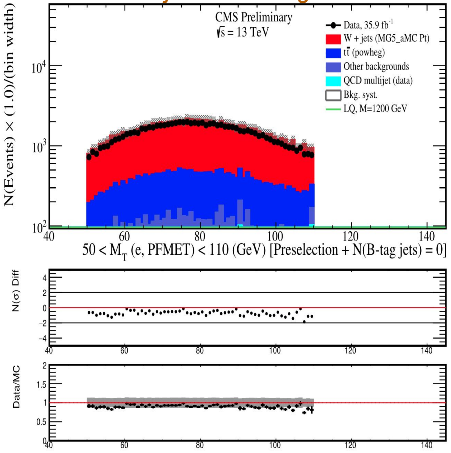

TTbar control region

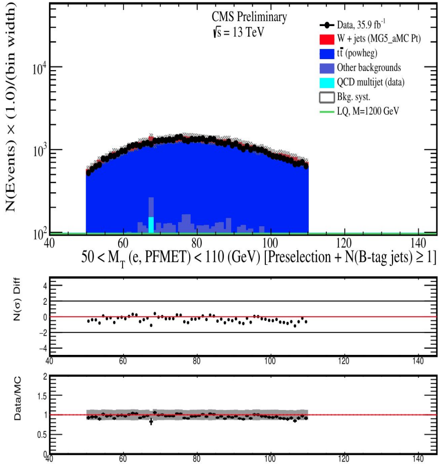

- Define a system of equations that can be solved to get the scale factors for W+jets and ttbar

$$\begin{cases} N^1_{\text{data}} = \mathcal{R}_{t\bar{t}} N^1_{t\bar{t}} + \mathcal{R}_W N^1_W + N^1_{\text{QCD}} + N^1_{\text{Others}} \\ N^2_{\text{data}} = \mathcal{R}_{t\bar{t}} N^2_{t\bar{t}} + \mathcal{R}_W N^2_W + N^2_{\text{QCD}} + N^2_{\text{Others}} \end{cases}$$

$$\mathcal{R}_{t\bar{t}} = 0.97 \pm 0.01$$
$$\mathcal{R}_W = 0.88 \pm 0.01$$

Preselection Distributions *evjj*

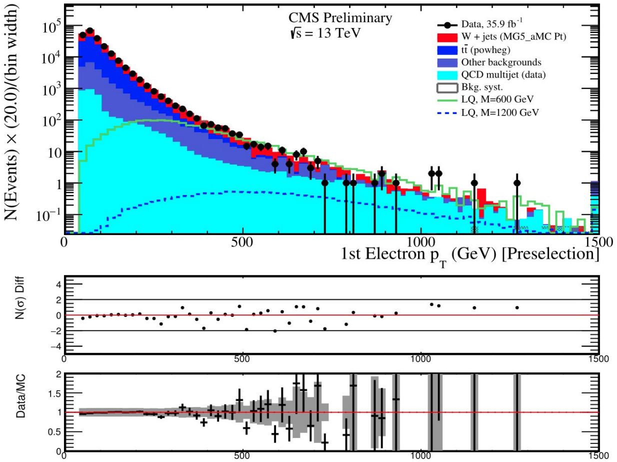

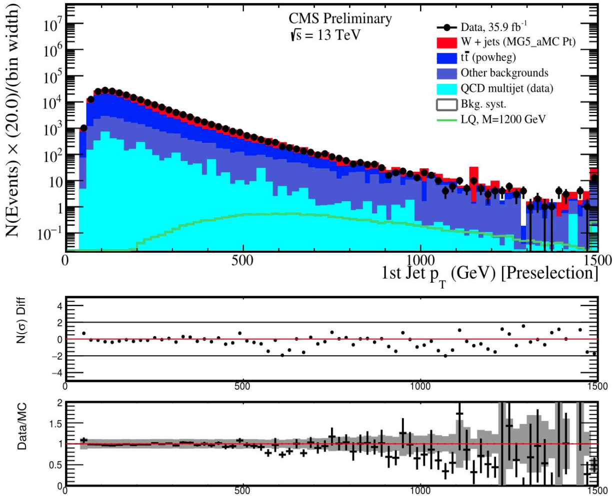

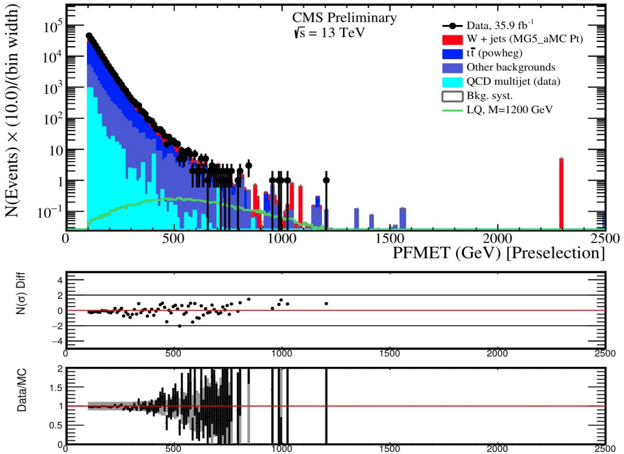

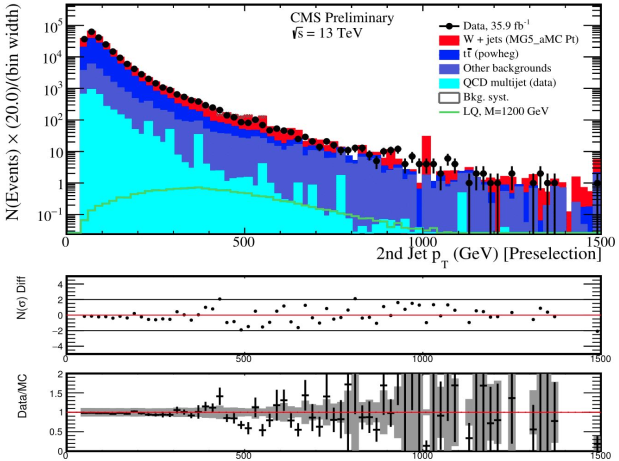

Kinematics of leptons and jets look well-modeled

Preselection Distributions *eνjj*

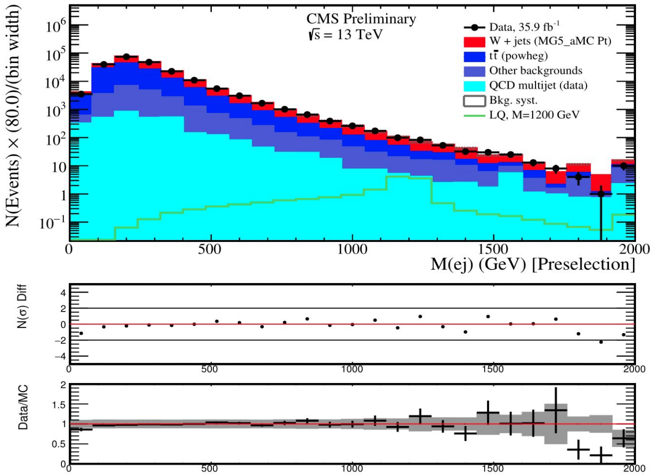

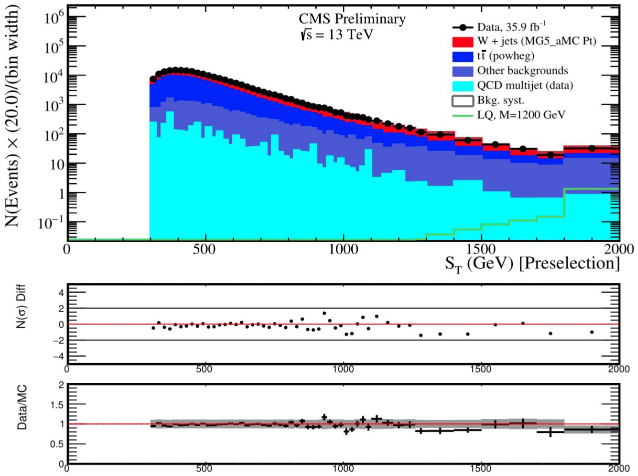

Selection variables also look good

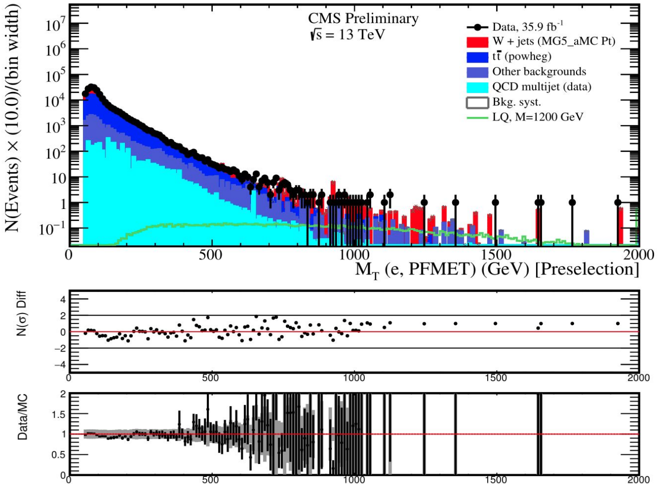

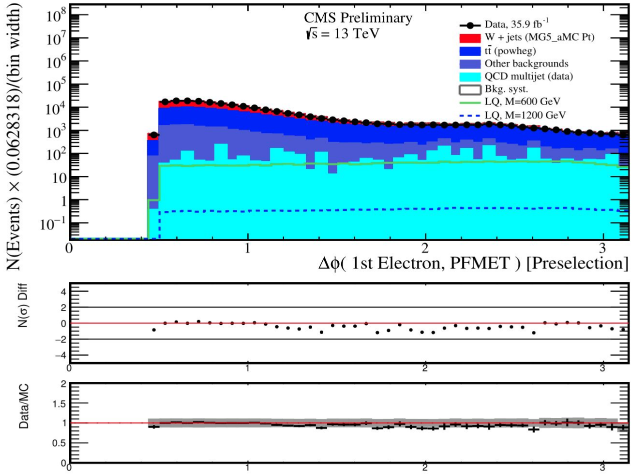

Systematics

Objects:

- JER/JES: nominal collections are shifted
- EER/EES:10%, 2% as recommended by EGamma POG
- Electron reconstruction efficiency: 5%
- Electron ID: 4% (6%) in barrel (endcap)
- MET: shift the JER, JES, electron energy and Unclustered energy

Detector:

- Luminosity: 2.5%

Simulation:

- Pileup (5%)
- PDF: shift nominal PDFs

Backgrounds:

- tt-bar, Z+jets and W+jets shape: vary renormalization/factorization scales
- tt-bar, Z+jets and W+jets normalisation: the stat. uncertainty on the scale factor is taken as the uncertainty on the normalisation
- QCD: 50%(eejj), 25%(*evjj)*

Expected Limits

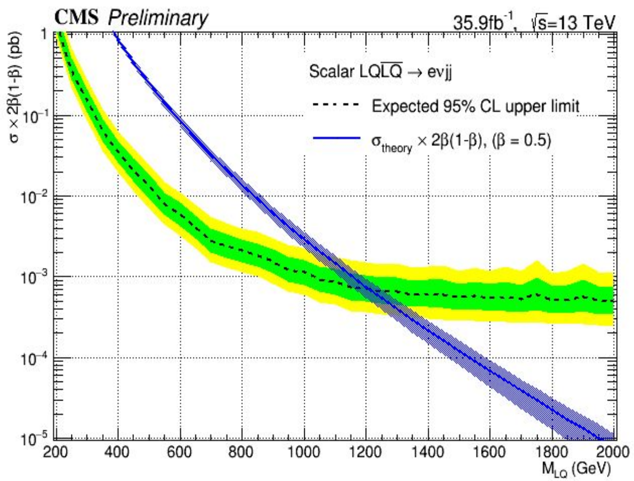

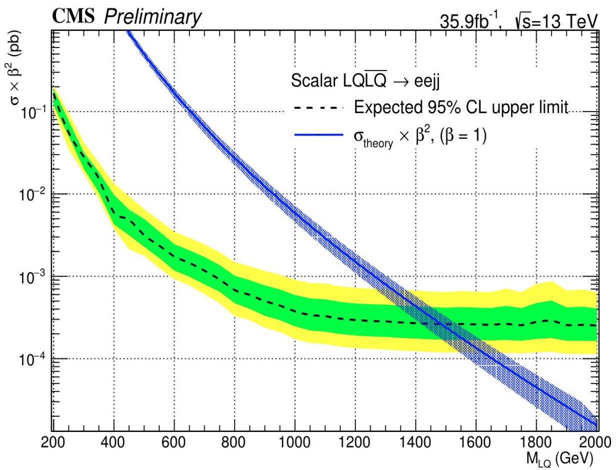

- 95% CL on $\sigma \times \beta^2$ (*eejj*) and $\sigma \times 2\beta(1-\beta)$(*evjj)*
- Expected mass limit:1490 GeV(*eejj*) and 1215 GeV (*evjj*)
- Limits on the LQ mass in *evjj* channel obtained for the first time at 13 TeV
- Calculated with asymptotic CL_s method
- 2015 data expected limit: 1130 GeV for *eejj*
- 8 TeV expected limit for *evjj* was 890 GeV

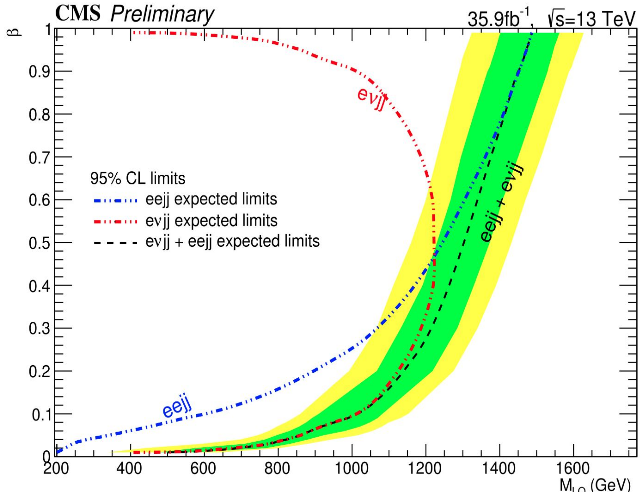

Conclusion

- A search for first generation pair produced scalar leptoquarks in the *eejj* and *eνjj* final state is conducted with the 13-TeV data recorded during 2016
- Set limits on $\sigma x \beta^2$ *(eejj)* and $\sigma \times 2\beta(1-\beta)$ *(eνjj)* as a function of the leptoquark mass; this results in a leptoquark mass limit of 1490 GeV *(eejj)* and 1215 GeV *(eνjj)*
- Expect to extend the eejj limits from 2015 by ~400 GeV, and set limits for *eνjj* for the first time at 13 TeV
- The analysis (EXO-17-009) is already pre-approved and now under active internal refereeing
- Expect it to be approved in next couple of weeks

Back up

Data and MC

signal →

Dataset	Run range
/SingleElectron_Run2016B-03Feb2017_ver2-v2/MINIAOD	272760-275376
/SingleElectron_Run2016C-03Feb2017-v1/MINIAOD	275656-276283
/SingleElectron_Run2016D-03Feb2017-v1/MINIAOD	276315-276811
/SingleElectron_Run2016E-03Feb2017-v1/MINIAOD	276831-277420
/SingleElectron_Run2016F-03Feb2017-v1/MINIAOD	277932-278808
/SingleElectron_Run2016G-03Feb2017-v1/MINIAOD	278820-280385
/SingleElectron_Run2016H-03Feb2017_ver2-v1/MINIAOD	281207-284035
/SingleElectron_Run2016H-03Feb2017_ver3-v1/MINIAOD	284036-284068
Integrated luminosity (Certified) $\mathcal{L} = 35.9\ \text{fb}^{-1}$	

Signal and QCD

Dataset	Run range
/SinglePhoton_Run2016B-03Feb2017_ver2-v2/MINIAOD	272760-275376
/SinglePhoton_Run2016C-03Feb2017-v1/MINIAOD	275656-276283
/SinglePhoton_Run2016D-03Feb2017-v1/MINIAOD	276315-276811
/SinglePhoton_Run2016E-03Feb2017-v1/MINIAOD	276831-277420
/SinglePhoton_Run2016F-03Feb2017-v1/MINIAOD	277932-278808
/SinglePhoton_Run2016G-03Feb2017-v1/MINIAOD	278820-280385
/SinglePhoton_Run2016H-03Feb2017_ver2-v1/MINIAOD	281207-284035
/SinglePhoton_Run2016H-03Feb2017_ver3-v1/MINIAOD	284036-284068
Integrated luminosity (Certified) $\mathcal{L} = 35.9\ \text{fb}^{-1}$	

JSON: /afs/cern.ch/cms/CAF/CMSCOMM/COMM DQM/certification/Collisions16/13TeV/ReReco/Final/Cert 271036-284044 13TeV 23Sep2016ReReco Collisions16 JSON.txt

MC Samples

RunIISummer16MiniAODv2_PUMoriond17_asymptotic, PU reweighting applied

DY, W+jets, Diboson → *MadGraph5_AMC@NLO*
Photon+jets → *MadGraph*
SingleTop → *Powheg*
TT+jets → *Powheg*

- *For data, we pick events from single electron dataset only if the event passes the single electron trigger but fails the single photon trigger, and pick events from the single photon dataset if the event fires the single photon trigger*

- ***Trigger*** : HLT_Ele27_WPTight_Gsf_v **OR** HLT_Ele115_CaloIdVT_GsfTrkIdT_v **OR** HLT_Photon175_v

Trigger efficiency with different combinations

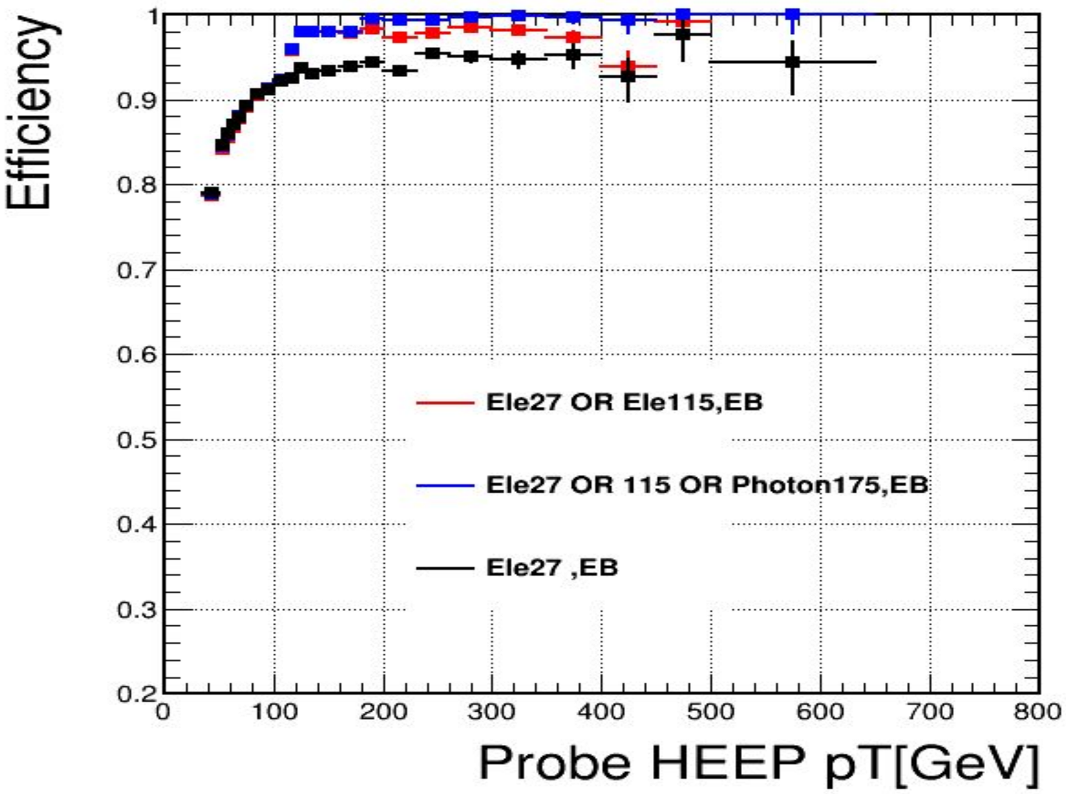

Optimisation (*eνjj*)

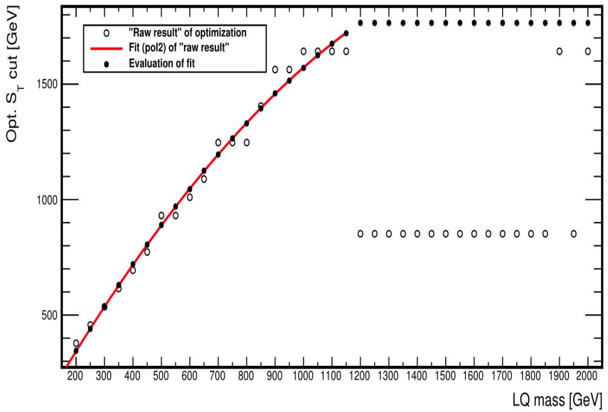

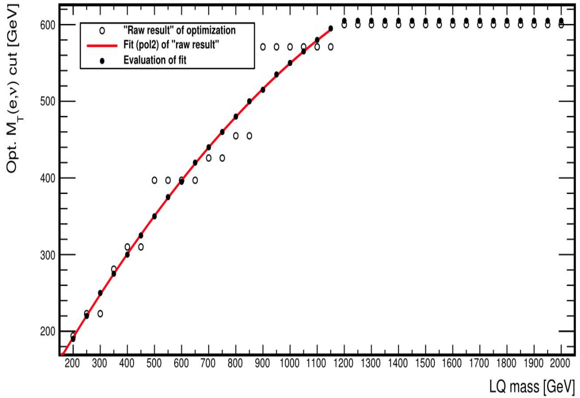

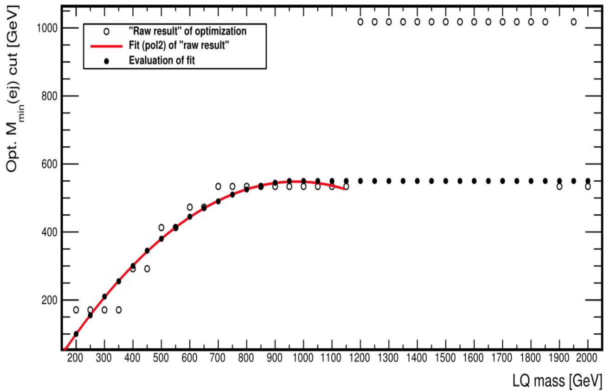

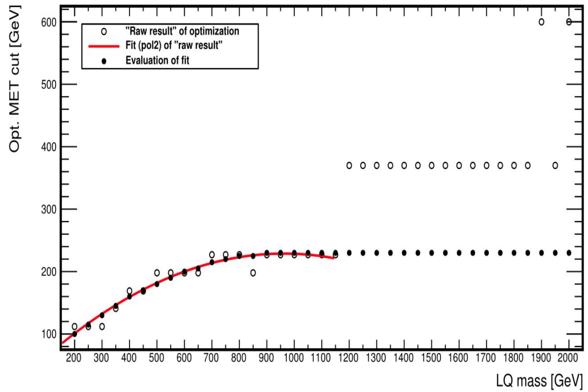

M_{LQ} [GeV]	S_T [GeV] $>$	$m_T(e,\nu)$ [GeV] $>$	E_T^{miss} [GeV] $>$	m_{ej} [GeV] $>$
200	345	190	100	100
250	440	220	115	155
300	535	250	130	210
350	630	275	145	255
400	720	300	160	300
450	805	325	170	345
500	890	350	180	380
550	970	375	190	415
600	1045	395	200	445
650	1125	420	205	470
700	1195	440	215	490
750	1265	460	220	510
800	1330	480	225	525
850	1395	500	225	535
900	1460	515	230	545
950	1515	535	230	550
1000	1570	550	230	550
1050	1625	565	230	550
1100	1675	580	230	550
1150	1720	595	230	550
$\geq$1200	1765	605	230	550

Optimisation (*eejj*)

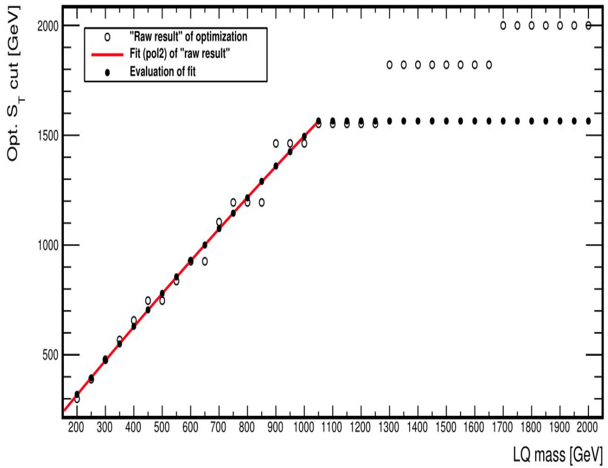

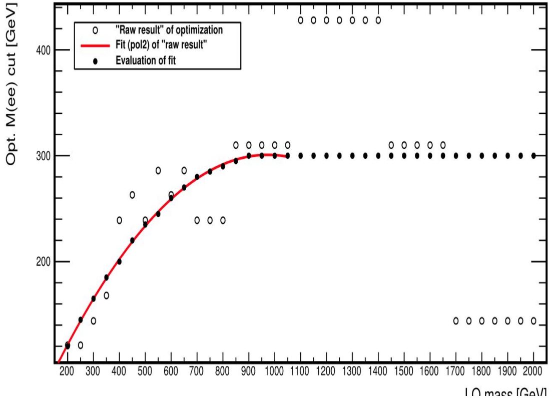

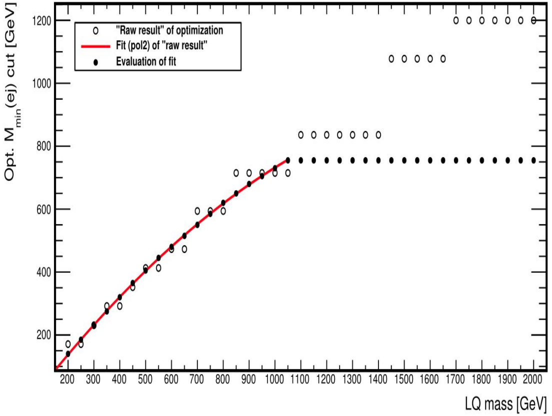

M_{LQ} [GeV]	S_T [GeV] >	m_{ee} [GeV] >	m_{ej}^{min} [GeV] >
200	320	120	140
250	395	145	185
300	475	165	230
350	550	185	275
400	630	200	320
450	705	220	365
500	780	235	405
550	855	245	445
600	930	260	480
650	1000	270	515
700	1075	280	550
750	1145	285	585
800	1215	290	620
850	1290	295	650
900	1360	300	680
950	1425	300	705
1000	1495	300	730
≥1050	1565	300	755

- Optimise the M_{ee}, S_T, M_{min}^{ej} by scanning the 3-D parameter space and maximising the Punzi criterion for each LQ mass hypothesis with a = 5

$$\frac{\epsilon(t)}{a/2 + \sqrt{B(t)}}$$

LQ signal samples

- LQ signal samples produced with Pythia8
- Mass range: 200-2000 GeV
- Pileup reweighting applied

M_{LQ}	$\sigma(\mu = M_{LQ})$ [pb]	$\delta(PDF)$	$\sigma(\mu = M_{LQ} \times 2)$ [pb]	$\sigma(\mu = M_{LQ}/2)$ [pb]
200	6.06E+01	2.50E+00	0.532E+02	0.683E+02
250	2.03E+01	1.09E+00	0.178E+02	0.228E+02
300	8.04E+00	5.35E-01	0.705E+01	0.902E+01
350	3.59E+00	2.85E-01	0.314E+01	0.401E+01
400	1.74E+00	1.61E-01	0.152E+01	0.194E+01
450	9.06E-01	9.52E-02	0.791E+00	0.101E+01
500	4.96E-01	5.78E-02	0.434E+00	0.553E+00
550	2.84E-01	3.69E-02	0.248E+00	0.316E+00
600	1.69E-01	2.37E-02	0.147E+00	0.188E+00
650	1.03E-01	1.57E-02	0.900E-01	0.115E+00
700	6.48E-02	1.06E-02	0.565E-01	0.721E-01
750	4.16E-02	7.27E-03	0.363E-01	0.463E-01
800	2.73E-02	5.03E-03	0.237E-01	0.303E-01
850	1.82E-02	3.55E-03	0.158E-01	0.202E-01
900	1.23E-02	2.53E-03	0.107E-01	0.137E-01
950	8.45E-03	1.83E-03	0.733E-02	0.939E-02
1000	5.86E-03	1.33E-03	0.508E-02	0.653E-02
1050	4.11E-03	9.82E-04	0.356E-02	0.458E-02
1100	2.91E-03	7.25E-04	0.252E-02	0.325E-02
1150	2.08E-03	5.41E-04	0.180E-02	0.232E-02
1200	1.50E-03	4.07E-04	0.129E-02	0.167E-02
1250	1.09E-03	3.09E-04	0.939E-03	0.122E-02
1300	7.95E-04	2.34E-04	0.684E-03	0.889E-03
1350	5.85E-04	1.79E-04	0.503E-03	0.654E-03
1400	4.33E-04	1.38E-04	0.371E-03	0.485E-03
1450	3.21E-04	1.06E-04	0.275E-03	0.360E-03
1500	2.40E-04	8.24E-05	0.205E-03	0.270E-03
1550	1.80E-04	6.43E-05	0.154E-03	0.202E-03
1600	1.35E-04	5.01E-05	0.115E-03	0.152E-03
1650	1.02E-04	3.92E-05	0.870E-04	0.115E-03
1700	7.74E-05	3.08E-05	0.658E-04	0.875E-04
1750	5.88E-05	2.43E-05	0.499E-04	0.666E-04
1800	4.48E-05	1.92E-05	0.380E-04	0.508E-04
1850	3.43E-05	1.52E-05	0.290E-04	0.389E-04
1900	2.62E-05	1.20E-05	0.221E-04	0.298E-04
1950	2.01E-05	9.55E-06	0.169E-04	0.230E-04
2000	1.55E-05	7.59E-06	0.130E-04	0.177E-04

MC Samples

Dataset	CrossSection (pb)
/DYJetsToLL_Zpt-0To50_TuneCUETP8M1_13TeV-amcatnloFXFX-pythia8/RunIISummer16MiniAODv2-PUMoriond17_80X_mcRun2_asymptotic_2016_TrancheIV_v6-v1/MINIAODSIM	5358.09
/DYJetsToLL_Pt-50To100_TuneCUETP8M1_13TeV-amcatnloFXFX-pythia8/RunIISummer16MiniAODv2-PUMoriond17_80X_mcRun2_asymptotic_2016_TrancheIV_v6-v3/MINIAODSIM	364.19
/DYJetsToLL_Pt-50To100_TuneCUETP8M1_13TeV-amcatnloFXFX-pythia8/RunIISummer16MiniAODv2-PUMoriond17_80X_mcRun2_asymptotic_2016_TrancheIV_v6_ext3-v1/MINIAODSIM	364.19
/DYJetsToLL_Pt-100To250_TuneCUETP8M1_13TeV-amcatnloFXFX-pythia8/RunIISummer16MiniAODv2-PUMoriond17_80X_mcRun2_asymptotic_2016_TrancheIV_v6-v2/MINIAODSIM	84.10
/DYJetsToLL_Pt-100To250_TuneCUETP8M1_13TeV-amcatnloFXFX-pythia8/RunIISummer16MiniAODv2-PUMoriond17_80X_mcRun2_asymptotic_2016_TrancheIV_v6_ext1-v1/MINIAODSIM	84.10
/DYJetsToLL_Pt-100To250_TuneCUETP8M1_13TeV-amcatnloFXFX-pythia8/RunIISummer16MiniAODv2-PUMoriond17_80X_mcRun2_asymptotic_2016_TrancheIV_v6_ext2-v1/MINIAODSIM	84.10
/DYJetsToLL_Pt-100To250_TuneCUETP8M1_13TeV-amcatnloFXFX-pythia8/RunIISummer16MiniAODv2-PUMoriond17_80X_mcRun2_asymptotic_2016_TrancheIV_v6_ext5-v1/MINIAODSIM	84.10
/DYJetsToLL_Pt-250To400_TuneCUETP8M1_13TeV-amcatnloFXFX-pythia8/RunIISummer16MiniAODv2-PUMoriond17_80X_mcRun2_asymptotic_2016_TrancheIV_v6-v1/MINIAODSIM	3.23
/DYJetsToLL_Pt-250To400_TuneCUETP8M1_13TeV-amcatnloFXFX-pythia8/RunIISummer16MiniAODv2-PUMoriond17_80X_mcRun2_asymptotic_2016_TrancheIV_v6_ext1-v1/MINIAODSIM	3.23
/DYJetsToLL_Pt-250To400_TuneCUETP8M1_13TeV-amcatnloFXFX-pythia8/RunIISummer16MiniAODv2-PUMoriond17_80X_mcRun2_asymptotic_2016_TrancheIV_v6_ext2-v1/MINIAODSIM	3.23
/DYJetsToLL_Pt-250To400_TuneCUETP8M1_13TeV-amcatnloFXFX-pythia8/RunIISummer16MiniAODv2-PUMoriond17_80X_mcRun2_asymptotic_2016_TrancheIV_v6_ext5-v1/MINIAODSIM	3.23
/DYJetsToLL_Pt-400To650_TuneCUETP8M1_13TeV-amcatnloFXFX-pythia8/RunIISummer16MiniAODv2-PUMoriond17_80X_mcRun2_asymptotic_2016_TrancheIV_v6-v1/MINIAODSIM	0.4365
/DYJetsToLL_Pt-400To650_TuneCUETP8M1_13TeV-amcatnloFXFX-pythia8/RunIISummer16MiniAODv2-PUMoriond17_80X_mcRun2_asymptotic_2016_TrancheIV_v6_ext1-v1/MINIAODSIM	0.4365
/DYJetsToLL_Pt-400To650_TuneCUETP8M1_13TeV-amcatnloFXFX-pythia8/RunIISummer16MiniAODv2-PUMoriond17_80X_mcRun2_asymptotic_2016_TrancheIV_v6_ext2-v1/MINIAODSIM	0.4365
/DYJetsToLL_Pt-650ToInf_TuneCUETP8M1_13TeV-amcatnloFXFX-pythia8/RunIISummer16MiniAODv2-PUMoriond17_80X_mcRun2_asymptotic_2016_TrancheIV_v6-v1/MINIAODSIM	0.0410
/DYJetsToLL_Pt-650ToInf_TuneCUETP8M1_13TeV-amcatnloFXFX-pythia8/RunIISummer16MiniAODv2-PUMoriond17_80X_mcRun2_asymptotic_2016_TrancheIV_v6_ext1-v1/MINIAODSIM	0.0410
/DYJetsToLL_Pt-650ToInf_TuneCUETP8M1_13TeV-amcatnloFXFX-pythia8/RunIISummer16MiniAODv2-PUMoriond17_80X_mcRun2_asymptotic_2016_TrancheIV_v6_ext2-v1/MINIAODSIM	0.0410
/TT_TuneCUETP8M2T4_13TeV-powheg-pythia8/RunIISummer16MiniAODv2-PUMoriond17_80X_mcRun2_asymptotic_2016_TrancheIV_v6-v1/MINIAODSIM	831.76
/TT_TuneCUETP8M2T4_13TeV-powheg-pythia8/RunIISummer16MiniAODv2-PUMoriond17_backup_80X_mcRun2_asymptotic_2016_TrancheIV_v6-v1/MINIAODSIM	831.76
/WJetsToLNu_Wpt-0To50_TuneCUETP8M1_13TeV-amcatnloFXFX-pythia8/RunIISummer16MiniAODv2-PUMoriond17_80X_mcRun2_asymptotic_2016_TrancheIV_v6-v1/MINIAODSIM	57319.92
/WJetsToLNu_Wpt-50To100_TuneCUETP8M1_13TeV-amcatnloFXFX-pythia8/RunIISummer16MiniAODv2-PUMoriond17_80X_mcRun2_asymptotic_2016_TrancheIV_v6-v1/MINIAODSIM	3299.67
/WJetsToLNu_Pt-100To250_TuneCUETP8M1_13TeV-amcatnloFXFX-pythia8/RunIISummer16MiniAODv2-PUMoriond17_80X_mcRun2_asymptotic_2016_TrancheIV_v6-v1/MINIAODSIM	690.02
/WJetsToLNu_Pt-100To250_TuneCUETP8M1_13TeV-amcatnloFXFX-pythia8/RunIISummer16MiniAODv2-PUMoriond17_80X_mcRun2_asymptotic_2016_TrancheIV_v6_ext1-v1/MINIAODSIM	690.02
/WJetsToLNu_Pt-100To250_TuneCUETP8M1_13TeV-amcatnloFXFX-pythia8/RunIISummer16MiniAODv2-PUMoriond17_80X_mcRun2_asymptotic_2016_TrancheIV_v6_ext4-v1/MINIAODSIM	690.02
/WJetsToLNu_Pt-250To400_TuneCUETP8M1_13TeV-amcatnloFXFX-pythia8/RunIISummer16MiniAODv2-PUMoriond17_80X_mcRun2_asymptotic_2016_TrancheIV_v6-v1/MINIAODSIM	24.52
/WJetsToLNu_Pt-250To400_TuneCUETP8M1_13TeV-amcatnloFXFX-pythia8/RunIISummer16MiniAODv2-PUMoriond17_80X_mcRun2_asymptotic_2016_TrancheIV_v6_ext1-v1/MINIAODSIM	24.52
/WJetsToLNu_Pt-250To400_TuneCUETP8M1_13TeV-amcatnloFXFX-pythia8/RunIISummer16MiniAODv2-PUMoriond17_80X_mcRun2_asymptotic_2016_TrancheIV_v6_ext4-v1/MINIAODSIM	24.52
/WJetsToLNu_Pt-400To600_TuneCUETP8M1_13TeV-amcatnloFXFX-pythia8/RunIISummer16MiniAODv2-PUMoriond17_80X_mcRun2_asymptotic_2016_TrancheIV_v6-v1/MINIAODSIM	3.11
/WJetsToLNu_Pt-400To600_TuneCUETP8M1_13TeV-amcatnloFXFX-pythia8/RunIISummer16MiniAODv2-PUMoriond17_80X_mcRun2_asymptotic_2016_TrancheIV_v6_ext1-v1/MINIAODSIM	3.11
/WJetsToLNu_Pt-600ToInf_TuneCUETP8M1_13TeV-amcatnloFXFX-pythia8/RunIISummer16MiniAODv2-PUMoriond17_80X_mcRun2_asymptotic_2016_TrancheIV_v6-v1/MINIAODSIM	0.4685
/WJetsToLNu_Pt-600ToInf_TuneCUETP8M1_13TeV-amcatnloFXFX-pythia8/RunIISummer16MiniAODv2-PUMoriond17_80X_mcRun2_asymptotic_2016_TrancheIV_v6_ext1-v1/MINIAODSIM	0.4685
/WWTo1L1Nu2Q_13TeV_amcatnloFXFX_madspin_pythia8/RunIISummer16MiniAODv2-PUMoriond17_80X_mcRun2_asymptotic_2016_TrancheIV_v6-v1/MINIAODSIM	45.68
/WWTo4Q_4f_13TeV_amcatnloFXFX_madspin_pythia8/RunIISummer16MiniAODv2-PUMoriond17_80X_mcRun2_asymptotic_2016_TrancheIV_v6-v1/MINIAODSIM	46.22
/WZTo1L1Nu2Q_13TeV_amcatnloFXFX_madspin_pythia8/RunIISummer16MiniAODv2-PUMoriond17_80X_mcRun2_asymptotic_2016_TrancheIV_v6-v3/MINIAODSIM	10.71
/WZTo1L3Nu_13TeV_amcatnloFXFX_madspin_pythia8/RunIISummer16MiniAODv2-PUMoriond17_80X_mcRun2_asymptotic_2016_TrancheIV_v6-v1/MINIAODSIM	3.033
/WZTo2L2Q_13TeV_amcatnloFXFX_madspin_pythia8/RunIISummer16MiniAODv2-PUMoriond17_80X_mcRun2_asymptotic_2016_TrancheIV_v6-v1/MINIAODSIM	5.595
/WZTo3LNu_TuneCUETP8M1_13TeV-amcatnloFXFX-pythia8/RunIISummer16MiniAODv2-PUMoriond17_80X_mcRun2_asymptotic_2016_TrancheIV_v6-v1/MINIAODSIM	5.26
/WZTo2Q2Nu_13TeV_amcatnloFXFX_madspin_pythia8/RunIISummer16MiniAODv2-PUMoriond17_80X_mcRun2_asymptotic_2016_TrancheIV_v6-v1/MINIAODSIM	6.324
/ZZTo2Q2Nu_13TeV_amcatnloFXFX_madspin_pythia8/RunIISummer16MiniAODv2-PUMoriond17_80X_mcRun2_asymptotic_2016_TrancheIV_v6-v1/MINIAODSIM	4.04
/ZZTo4L_13TeV-amcatnloFXFX-pythia8/RunIISummer16MiniAODv2-PUMoriond17_80X_mcRun2_asymptotic_2016_TrancheIV_v6_ext1-v1/MINIAODSIM	1.212
/ZZTo4Q_13TeV_amcatnloFXFX_madspin_pythia8/RunIISummer16MiniAODv2-PUMoriond17_80X_mcRun2_asymptotic_2016_TrancheIV_v6-v1/MINIAODSIM	6.904
/ZZTo2L2Q_13TeV_amcatnloFXFX_madspin_pythia8/RunIISummer16MiniAODv2-PUMoriond17_80X_mcRun2_asymptotic_2016_TrancheIV_v6-v1/MINIAODSIM	3.22
/VVTo2L2Nu_13TeV_amcatnloFXFX_madspin_pythia8/RunIISummer16MiniAODv2-PUMoriond17_80X_mcRun2_asymptotic_2016_TrancheIV_v6-v1/MINIAODSIM	11.95
/ST_s-channel_4f_InclusiveDecays_13TeV-amcatnlo-pythia8/RunIISummer16MiniAODv2-PUMoriond17_80X_mcRun2_asymptotic_2016_TrancheIV_v6-v1/MINIAODSIM	10.1
/ST_t-channel_antitop_4f_inclusiveDecays_TuneCUETP8M2T4_13TeV-powhegV2-madspin/RunIISummer16MiniAODv2-PUMoriond17_80X_mcRun2_asymptotic_2016_TrancheIV_v6-v1/MINIAODSIM	81.0
/ST_t-channel_top_4f_inclusiveDecays_TuneCUETP8M2T4_13TeV-powhegV2-madspin/RunIISummer16MiniAODv2-PUMoriond17_80X_mcRun2_asymptotic_2016_TrancheIV_v6-v1/MINIAODSIM	136.0
/ST_tW_antitop_5f_inclusiveDecays_13TeV-powheg-pythia8_TuneCUETP8M2T4/RunIISummer16MiniAODv2-PUMoriond17_80X_mcRun2_asymptotic_2016_TrancheIV_v6-v1/MINIAODSIM	35.6
/ST_tW_top_5f_inclusiveDecays_13TeV-powheg-pythia8_TuneCUETP8M2T4/RunIISummer16MiniAODv2-PUMoriond17_80X_mcRun2_asymptotic_2016_TrancheIV_v6-v1/MINIAODSIM	35.6
/GJets_HT-40To100_TuneCUETP8M1_13TeV-madgraphMLM-pythia8/RunIISummer16MiniAODv2-PUMoriond17_80X_mcRun2_asymptotic_2016_TrancheIV_v6-v1/MINIAODSIM	20730.0
/GJets_HT-40To100_TuneCUETP8M1_13TeV-madgraphMLM-pythia8/RunIISummer16MiniAODv2-PUMoriond17_80X_mcRun2_asymptotic_2016_TrancheIV_v6_ext1-v1/MINIAODSIM	20730.0
/GJets_HT-100To200_TuneCUETP8M1_13TeV-madgraphMLM-pythia8/RunIISummer16MiniAODv2-PUMoriond17_80X_mcRun2_asymptotic_2016_TrancheIV_v6-v1/MINIAODSIM	9238.0
/GJets_HT-100To200_TuneCUETP8M1_13TeV-madgraphMLM-pythia8/RunIISummer16MiniAODv2-PUMoriond17_80X_mcRun2_asymptotic_2016_TrancheIV_v6_ext1-v1/MINIAODSIM	9238.0
/GJets_HT-200To400_TuneCUETP8M1_13TeV-madgraphMLM-pythia8/RunIISummer16MiniAODv2-PUMoriond17_80X_mcRun2_asymptotic_2016_TrancheIV_v6-v1/MINIAODSIM	2305.0
/GJets_HT-200To400_TuneCUETP8M1_13TeV-madgraphMLM-pythia8/RunIISummer16MiniAODv2-PUMoriond17_80X_mcRun2_asymptotic_2016_TrancheIV_v6_ext1-v1/MINIAODSIM	2305.0
/GJets_HT-400To600_TuneCUETP8M1_13TeV-madgraphMLM-pythia8/RunIISummer16MiniAODv2-PUMoriond17_80X_mcRun2_asymptotic_2016_TrancheIV_v6-v1/MINIAODSIM	274.4
/GJets_HT-400To600_TuneCUETP8M1_13TeV-madgraphMLM-pythia8/RunIISummer16MiniAODv2-PUMoriond17_80X_mcRun2_asymptotic_2016_TrancheIV_v6_ext1-v2/MINIAODSIM	274.4
/GJets_HT-600ToInf_TuneCUETP8M1_13TeV-madgraphMLM-pythia8/RunIISummer16MiniAODv2-PUMoriond17_80X_mcRun2_asymptotic_2016_TrancheIV_v6-v1/MINIAODSIM	93.5
/GJets_HT-600ToInf_TuneCUETP8M1_13TeV-madgraphMLM-pythia8/RunIISummer16MiniAODv2-PUMoriond17_80X_mcRun2_asymptotic_2016_TrancheIV_v6_ext1-v1/MINIAODSIM	93.5

Negative weight event

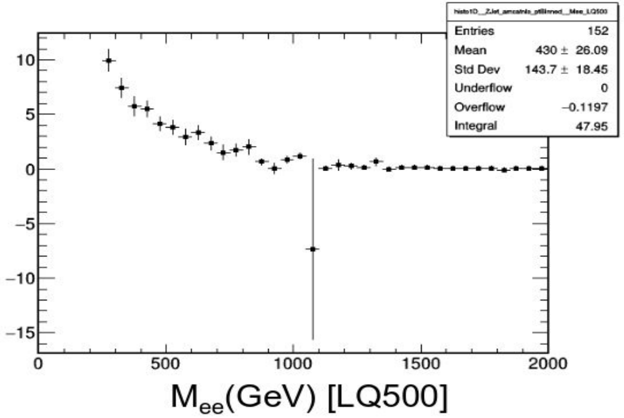

Comes from DYJets Pt-0To50
Gets cut out at $M_{LQ} \geq$ 550 GeV selections by Mej_min cut
Pt(ee) ~ 60 GeV
Mej_min ~ 380 GeV
sT(eej) ~ 1050 GeV

Try applying Pt(ee) > 70 GeV to cut out the mainly negative weight events from this sample

QCD fake rate

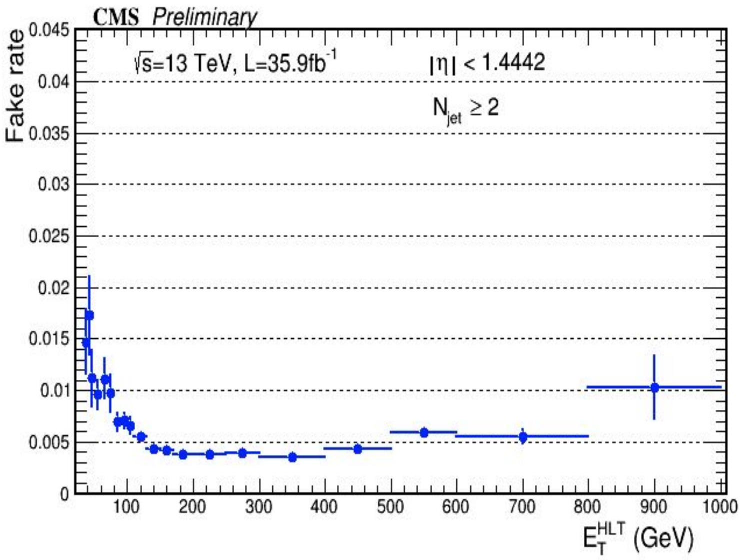

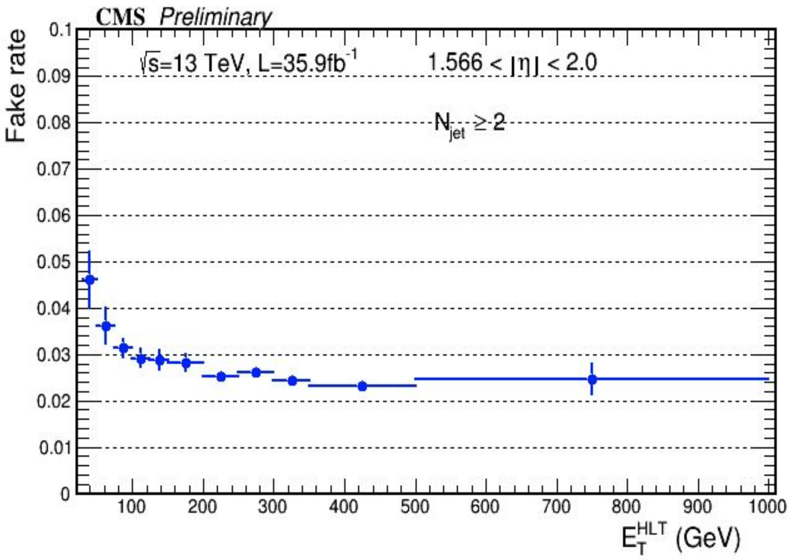

- Fake-rate for N_{jet} >=2

Fakerate for Njet >=2, eta > 2.0

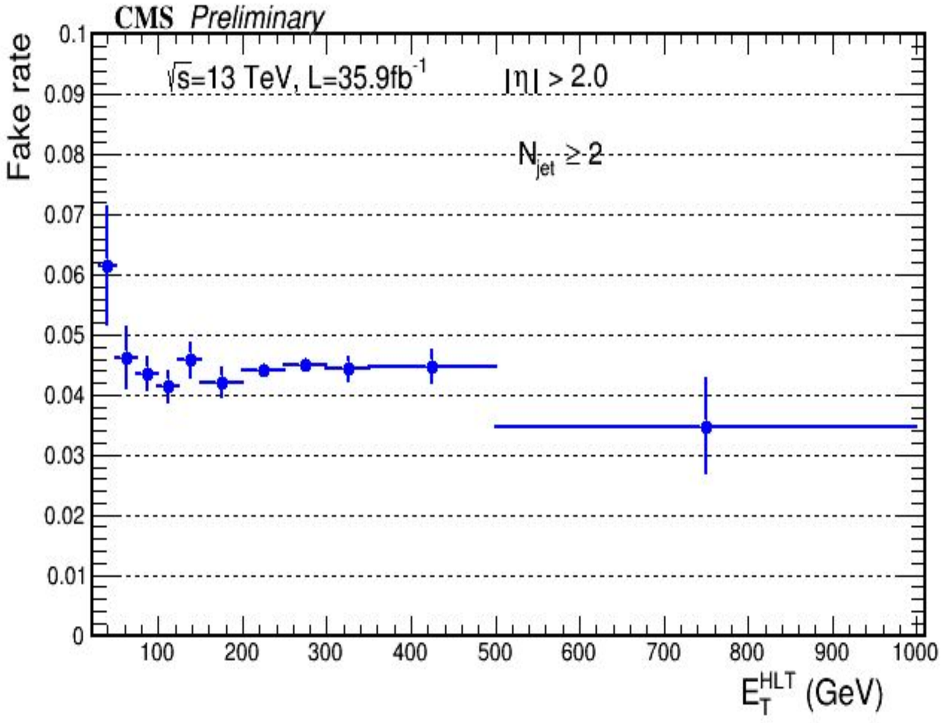

Comparison of fakerate with Z' results

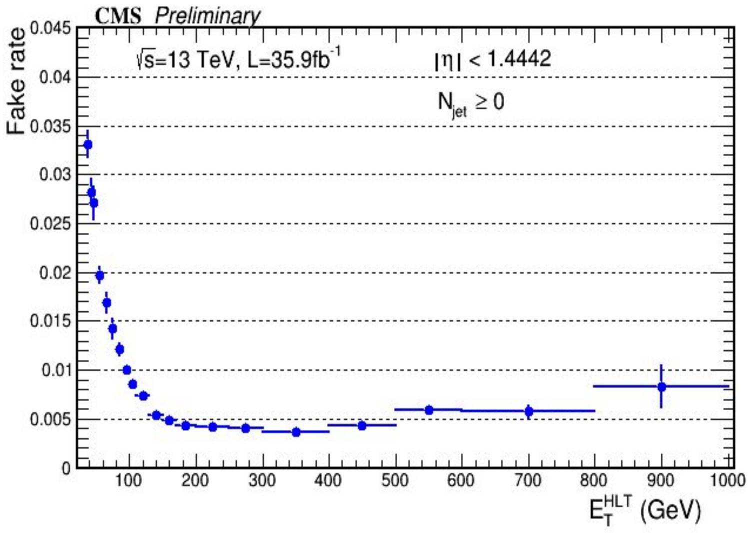

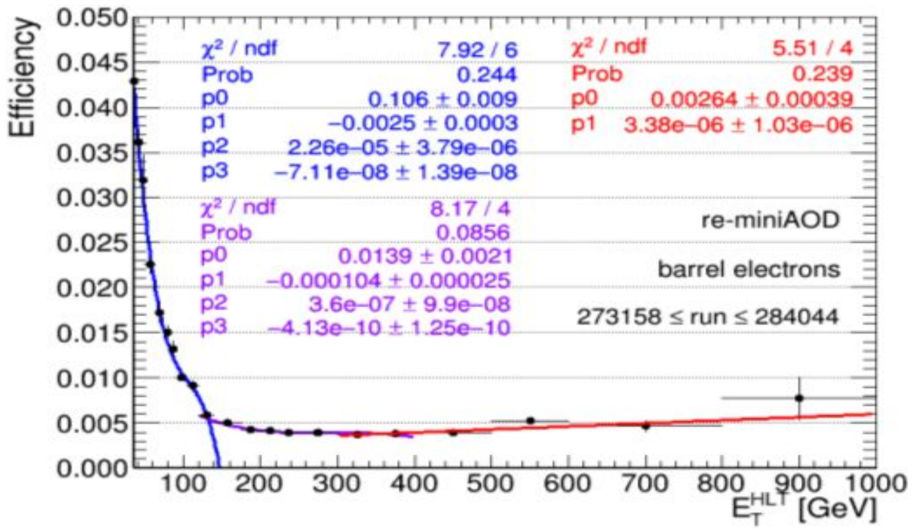

Z' results

Negative fakerate

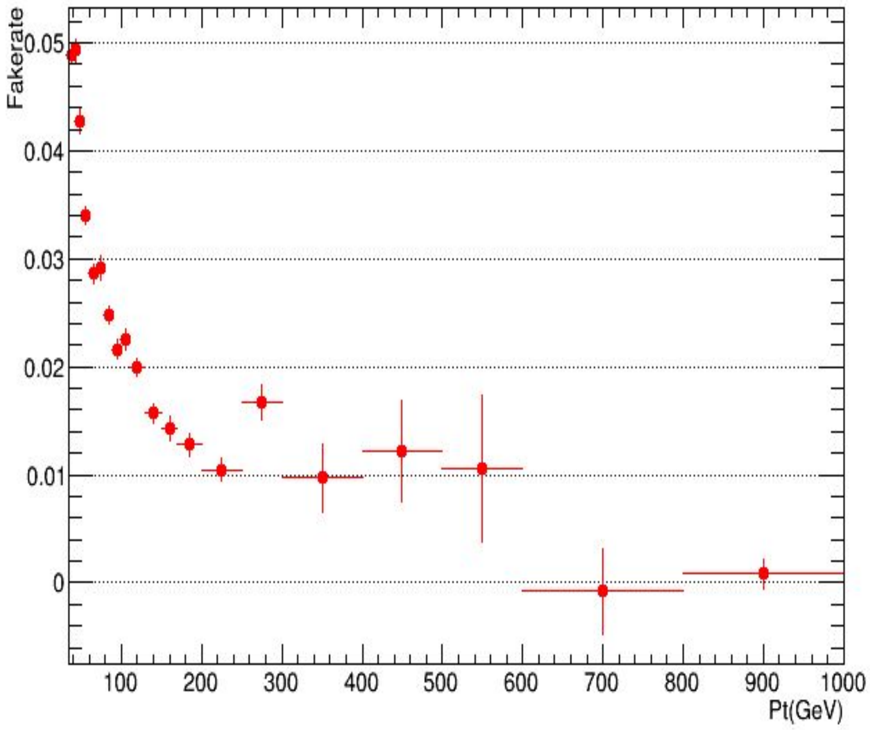

Systematics (LQ1000)

Table 3: Systematic uncertainties for the $eejj$ and $e\nu jj$ channel (LQ 1000)

Systematic	$eejj$ Signal (%)	$eejj$ Background (%)	$e\nu jj$ Signal (%)	$e\nu jj$ Background (%)
Electron reco efficiency	2.99	2.96	0.59	0.83
Electron Energy Scale	1.54	2.47	1.93	6.86
Electron Energy Resolution	2.72	5.27	0.07	4.87
Trigger	1.14	1.36	9.5	7.62
HEEP ID efficiency	1.30	0.32	0.62	0.13
Jet Energy Scale	0.48	0.91	0.49	2.32
Jet Energy Resolution	0.11	1.69	0.09	2.42
Luminosity	2.50	0.62	2.50	0.53
Pileup	0.17	1.02	0.43	1.42
PDF	2.81	3.01	2.93	4.7
DY + jets Shape	-	5.56	-	-
MET	-	-	0.80	13.1
W Shape	-	-	-	7.05
TT Shape	-	-	-	10.37
DY Normalisation	-	1.03	-	-
W Normalisation	-	-	-	1.14
TT Normalisation	-	-	-	1.03
W Norm. from variation of MT	-	-	-	10.0
W Norm. from variation of B-tag SF's	-	-	-	3.0
TT Norm. from variation of B-tag SF's	-	-	-	3.0

Event Yield (eejj)

M_{LQ}	LQ Signal	Z+Jets	$t\bar{t}$	QCD (data)	Diboson	ST	W+Jets	G+Jets	Total BG (stat) (syst)	Data
preselection	–	41592.2 ± 43.52	7011.8 ± 72.05	25.78 ± 0.12	1633.42 ± 4.15	495.65 ± 9.2	175.96 ± 32.08	67.74 ± 13.76	$51002.57 \pm 91.68 \pm 2672.04$	50594.0
200	311548.18 ± 3272.15	1851.31 ± 14.83	2297.0 ± 41.0	14.67 ± 0.09	255.7 ± 2.5	242.77 ± 6.45	92.68 ± 11.44	37.65 ± 10.94	$4791.79 \pm 46.9 \pm 126.91$	4710.0
250	137384.34 ± 1220.19	898.66 ± 10.76	1233.28 ± 30.28	9.11 ± 0.06	156.28 ± 2.13	143.83 ± 4.96	55.06 ± 11.07	20.82 ± 7.45	$2517.05 \pm 35.21 \pm 70.72$	2426.0
300	63160.43 ± 511.57	466.61 ± 3.56	612.83 ± 22.52	4.75 ± 0.04	94.78 ± 1.7	84.2 ± 3.83	32.32 ± 7.37	$12.83^{+5.86}_{-4.2}$	$1308.32^{+25.02}_{-24.68} \pm 27.29$	1278.0
350	30151.87 ± 232.77	248.68 ± 2.39	301.43 ± 16.02	2.52 ± 0.03	58.65 ± 1.48	50.37 ± 2.96	24.95 ± 7.29	$7.52^{+5.09}_{-3.25}$	$694.12^{+18.77}_{-18.36} \pm 27.86$	652.0
400	15436.95 ± 114.62	143.4 ± 1.71	145.47 ± 11.65	1.02 ± 0.01	36.93 ± 1.2	32.62 ± 2.38	15.13 ± 4.92	$4.71^{+4.58}_{-2.56}$	$379.28^{+13.82}_{-13.29} \pm 12.0$	376.0
450	8256.38 ± 60.38	86.76 ± 1.37	73.68 ± 8.38	0.57 ± 0.01	23.29 ± 1.04	19.99 ± 1.87	5.84 ± 0.89	$0.0^{+0.33}_{-0}$	$210.13^{+8.8}_{-8.8} \pm 6.48$	209.0
500	4704.25 ± 33.31	55.42 ± 1.06	31.34 ± 6.11	0.34 ± 0.01	15.62 ± 0.95	12.36 ± 1.48	2.29 ± 0.66	$0.0^{+0.36}_{-0}$	$117.37^{+6.49}_{-6.48} \pm 4.97$	128.0
550	2827.85 ± 19.38	33.97 ± 0.7	15.06 ± 4.49	0.22 ± 0.01	10.49 ± 0.71	9.7 ± 1.32	1.56 ± 0.9	$0.0^{+0.35}_{-0}$	$71.01^{+4.88}_{-4.87} \pm 3.05$	84.0
600	1754.86 ± 11.66	22.09 ± 0.56	9.57 ± 3.69	0.14 ± 0.005	7.67 ± 0.66	7.06 ± 1.13	1.11 ± 0.82	$0.0^{+0.32}_{-0}$	$47.64^{+4.06}_{-4.04} \pm 2.21$	58.0
650	1109.9 ± 7.21	15.54 ± 0.47	9.25 ± 3.08	0.07 ± 0.003	5.77 ± 0.63	4.25 ± 0.87	0.86 ± 0.78	$0.0^{+0.28}_{-0}$	$35.75^{+3.4}_{-3.39} \pm 1.58$	37.0
700	718.07 ± 4.54	11.7 ± 0.43	3.91 ± 2.46	0.06 ± 0.003	3.67 ± 0.57	2.84 ± 0.71	0.84 ± 0.78	$0.0^{+0.24}_{-0}$	$23.02^{+2.78}_{-2.77} \pm 1.17$	28.0
750	474.62 ± 2.94	7.7 ± 0.32	2.06 ± 2.01	0.04 ± 0.003	2.84 ± 0.54	2.27 ± 0.63	0.39 ± 0.72	$0.0^{+0.21}_{-0}$	$15.3^{+2.32}_{-2.31} \pm 0.74$	17.0
800	321.35 ± 1.94	6.31 ± 0.33	$1.18^{+0.58}_{-0.41}$	0.03 ± 0.002	1.74 ± 0.21	$1.72^{+0.73}_{-0.53}$	0.01 ± 0.69	$0.0^{+0.17}_{-0}$	$10.99^{+1.24}_{-1.04} \pm 0.67$	13.0
850	221.28 ± 1.31	4.93 ± 0.28	$1.23^{+0.66}_{-0.45}$	0.02 ± 0.002	1.33 ± 0.17	$1.51^{+0.74}_{-0.52}$	$0.0^{+0.68}_{-0.0}$	$0.0^{+0.14}_{-0}$	$9.02^{+1.26}_{-0.77} \pm 0.53$	10.0
900	153.04 ± 0.89	4.05 ± 0.28	$0.0^{+1.1}_{-0.0}$	0.01 ± 0.001	0.97 ± 0.13	$1.31^{+0.71}_{-0.48}$	$0.36^{+0.2}_{-0.13}$	$0.0^{+0.12}_{-0}$	$6.7^{+1.36}_{-0.59} \pm 0.44$	8.0
950	108.47 ± 0.61	3.16 ± 0.34	$0.0^{+0.88}_{-0.0}$	0.01 ± 0.001	0.8 ± 0.14	$0.94^{+0.64}_{-0.41}$	$0.36^{+0.2}_{-0.13}$	$0.0^{+0.1}_{-0}$	$5.27^{+1.16}_{-0.56} \pm 0.35$	5.0
1000	76.76 ± 0.43	2.06 ± 0.12	$0.0^{+0.65}_{-0.0}$	0.01 ± 0.001	0.56 ± 0.11	$0.94^{+0.64}_{-0.41}$	$0.36^{+0.2}_{-0.13}$	$0.0^{+0.08}_{-0}$	$3.93^{+0.94}_{-0.46} \pm 0.26$	5.0
1050	55.43 ± 0.3	1.73 ± 0.09	$0.0^{+0.32}_{-0.0}$	0.01 ± 0.001	0.31 ± 0.06	$0.76^{+0.6}_{-0.36}$	$0.34^{+0.2}_{-0.14}$	$0.0^{+0.06}_{-0}$	$3.15^{+0.72}_{-0.4} \pm 0.22$	4.0
1100	41.01 ± 0.21	1.73 ± 0.09	$0.0^{+0.32}_{-0.0}$	0.01 ± 0.001	0.31 ± 0.06	$0.76^{+0.6}_{-0.36}$	$0.34^{+0.2}_{-0.14}$	$0.0^{+0.06}_{-0}$	$3.15^{+0.72}_{-0.4} \pm 0.22$	4.0
1150	31.16 ± 0.15	1.73 ± 0.09	$0.0^{+0.32}_{-0.0}$	0.01 ± 0.001	0.31 ± 0.06	$0.76^{+0.6}_{-0.36}$	$0.34^{+0.2}_{-0.14}$	$0.0^{+0.06}_{-0}$	$3.15^{+0.72}_{-0.4} \pm 0.22$	4.0
1200	23.38 ± 0.11	1.73 ± 0.09	$0.0^{+0.32}_{-0.0}$	0.01 ± 0.001	0.31 ± 0.06	$0.76^{+0.6}_{-0.36}$	$0.34^{+0.2}_{-0.14}$	$0.0^{+0.06}_{-0}$	$3.15^{+0.72}_{-0.4} \pm 0.24$	4.0
1250	17.42 ± 0.08	1.73 ± 0.09	$0.0^{+0.32}_{-0.0}$	0.01 ± 0.001	0.31 ± 0.06	$0.76^{+0.6}_{-0.36}$	$0.34^{+0.2}_{-0.14}$	$0.0^{+0.06}_{-0}$	$3.15^{+0.72}_{-0.4} \pm 0.24$	4.0
1300	12.99 ± 0.06	1.73 ± 0.09	$0.0^{+0.32}_{-0.0}$	0.01 ± 0.001	0.31 ± 0.06	$0.76^{+0.6}_{-0.36}$	$0.34^{+0.2}_{-0.14}$	$0.0^{+0.06}_{-0}$	$3.15^{+0.72}_{-0.4} \pm 0.24$	4.0
1350	9.77 ± 0.04	1.73 ± 0.09	$0.0^{+0.32}_{-0.0}$	0.01 ± 0.001	0.31 ± 0.06	$0.76^{+0.6}_{-0.36}$	$0.34^{+0.2}_{-0.14}$	$0.0^{+0.06}_{-0}$	$3.15^{+0.72}_{-0.4} \pm 0.24$	4.0
1400	7.37 ± 0.03	1.73 ± 0.09	$0.0^{+0.32}_{-0.0}$	0.01 ± 0.001	0.31 ± 0.06	$0.76^{+0.6}_{-0.36}$	$0.34^{+0.2}_{-0.14}$	$0.0^{+0.06}_{-0}$	$3.15^{+0.72}_{-0.4} \pm 0.24$	4.0
1450	5.59 ± 0.02	1.73 ± 0.09	$0.0^{+0.32}_{-0.0}$	0.01 ± 0.001	0.31 ± 0.06	$0.76^{+0.6}_{-0.36}$	$0.34^{+0.2}_{-0.14}$	$0.0^{+0.06}_{-0}$	$3.15^{+0.72}_{-0.4} \pm 0.24$	4.0
1500	4.22 ± 0.02	1.73 ± 0.09	$0.0^{+0.32}_{-0.0}$	0.01 ± 0.001	0.31 ± 0.06	$0.76^{+0.6}_{-0.36}$	$0.34^{+0.2}_{-0.14}$	$0.0^{+0.06}_{-0}$	$3.15^{+0.72}_{-0.4} \pm 0.24$	4.0
1550	3.18 ± 0.01	1.73 ± 0.09	$0.0^{+0.32}_{-0.0}$	0.01 ± 0.001	0.31 ± 0.06	$0.76^{+0.6}_{-0.36}$	$0.34^{+0.2}_{-0.14}$	$0.0^{+0.06}_{-0}$	$3.15^{+0.72}_{-0.4} \pm 0.24$	4.0
1600	2.4 ± 0.01	1.73 ± 0.09	$0.0^{+0.32}_{-0.0}$	0.01 ± 0.001	0.31 ± 0.06	$0.76^{+0.6}_{-0.36}$	$0.34^{+0.2}_{-0.14}$	$0.0^{+0.06}_{-0}$	$3.15^{+0.72}_{-0.4} \pm 0.24$	4.0
1650	1.84 ± 0.01	1.73 ± 0.09	$0.0^{+0.32}_{-0.0}$	0.01 ± 0.001	0.31 ± 0.06	$0.76^{+0.6}_{-0.36}$	$0.34^{+0.2}_{-0.14}$	$0.0^{+0.06}_{-0}$	$3.15^{+0.72}_{-0.4} \pm 0.24$	4.0
1700	1.41 ± 0.01	1.73 ± 0.09	$0.0^{+0.32}_{-0.0}$	0.01 ± 0.001	0.31 ± 0.06	$0.76^{+0.6}_{-0.36}$	$0.34^{+0.2}_{-0.14}$	$0.0^{+0.06}_{-0}$	$3.15^{+0.72}_{-0.4} \pm 0.24$	4.0
1750	1.07 ± 0.004	1.73 ± 0.09	$0.0^{+0.32}_{-0.0}$	0.01 ± 0.001	0.31 ± 0.06	$0.76^{+0.6}_{-0.36}$	$0.34^{+0.2}_{-0.14}$	$0.0^{+0.06}_{-0}$	$3.15^{+0.72}_{-0.4} \pm 0.24$	4.0
1800	0.81 ± 0.003	1.73 ± 0.09	$0.0^{+0.32}_{-0.0}$	0.01 ± 0.001	0.31 ± 0.06	$0.76^{+0.6}_{-0.36}$	$0.34^{+0.2}_{-0.14}$	$0.0^{+0.06}_{-0}$	$3.15^{+0.72}_{-0.4} \pm 0.24$	4.0
1850	0.63 ± 0.003	1.73 ± 0.09	$0.0^{+0.32}_{-0.0}$	0.01 ± 0.001	0.31 ± 0.06	$0.76^{+0.6}_{-0.36}$	$0.34^{+0.2}_{-0.14}$	$0.0^{+0.06}_{-0}$	$3.15^{+0.72}_{-0.4} \pm 0.24$	4.0
1900	0.48 ± 0.002	1.73 ± 0.09	$0.0^{+0.32}_{-0.0}$	0.01 ± 0.001	0.31 ± 0.06	$0.76^{+0.6}_{-0.36}$	$0.34^{+0.2}_{-0.14}$	$0.0^{+0.06}_{-0}$	$3.15^{+0.72}_{-0.4} \pm 0.24$	4.0
1950	0.37 ± 0.001	1.73 ± 0.09	$0.0^{+0.32}_{-0.0}$	0.01 ± 0.001	0.31 ± 0.06	$0.76^{+0.6}_{-0.36}$	$0.34^{+0.2}_{-0.14}$	$0.0^{+0.06}_{-0}$	$3.15^{+0.72}_{-0.4} \pm 0.24$	4.0
2000	0.29 ± 0.001	1.73 ± 0.09	$0.0^{+0.32}_{-0.0}$	0.01 ± 0.001	0.31 ± 0.06	$0.76^{+0.6}_{-0.36}$	$0.34^{+0.2}_{-0.14}$	$0.0^{+0.06}_{-0}$	$3.15^{+0.72}_{-0.4} \pm 0.24$	4.0

Event Yield (*evjj*)

M_{LQ}	LQ Signal	W+Jets	$t\bar{t}$	QCD (data)	Diboson	ST	Z+Jets	G+Jets	Total BG (stat) (syst)	Data
preselection	–	47791.73 ± 153.85	67299.41 ± 106.13	2866.18 ± 14.86	2880.49 ± 17.99	6290.99 ± 30.2	888.44 ± 19.45	1372.85 ± 69.93	129390.09 ± 204.11 ± 8935.85	125487.0
200	130866.78 ± 1556.0	40107.11 ± 140.96	53108.4 ± 94.33	2122.27 ± 10.95	2543.79 ± 16.95	5267.29 ± 27.65	765.62 ± 17.74	1148.58 ± 55.85	105063.05 ± 182.69 ± 7376.89	101916.0
250	44362.2 ± 524.28	1755.44 ± 25.58	3782.36 ± 25.23	298.67 ± 2.3	503.35 ± 5.4	459.62 ± 8.89	106.82 ± 8.85	249.71 ± 37.16	7155.98 ± 53.51 ± 470.52	7192.0
300	19830.96 ± 217.05	828.5 ± 18.59	1455.61 ± 15.7	118.54 ± 1.34	277.83 ± 4.31	217.99 ± 6.16	48.98 ± 8.73	124.38 ± 35.23	3071.83 ± 44.36 ± 203.97	3174.0
350	9845.74 ± 101.23	411.43 ± 14.55	623.34 ± 10.3	61.66 ± 0.99	158.69 ± 3.33	116.52 ± 4.51	27.98 ± 8.7	70.63 ± 34.36	1470.25 ± 40.08 ± 106.55	1544.0
400	5134.02 ± 50.77	231.0 ± 10.06	309.98 ± 7.31	37.35 ± 0.81	94.76 ± 2.36	64.0 ± 3.34	18.68 ± 8.68	17.08 ± 3.23	772.85 ± 16.06 ± 85.75	851.0
450	2893.74 ± 27.09	147.53 ± 5.86	160.77 ± 5.27	28.03 ± 0.78	57.27 ± 1.72	39.49 ± 2.63	15.44 ± 8.68	9.75 ± 2.6	458.29 ± 12.44 ± 41.5	497.0
500	1654.01 ± 15.13	88.39 ± 3.75	90.44 ± 3.96	21.14 ± 0.8	38.13 ± 1.42	28.14 ± 2.23	4.11 ± 0.28	$6.18^{+2.82}_{-2.02}$	$276.53^{+6.74}_{-6.44}$ ± 29.33	299.0
550	988.65 ± 8.8	59.31 ± 5.17	50.69 ± 2.96	9.06 ± 0.41	26.28 ± 1.16	17.95 ± 1.76	2.3 ± 0.17	$5.51^{+2.72}_{-1.91}$	$171.1^{+6.9}_{-6.62}$ ± 19.17	195.0
600	616.38 ± 5.34	45.0 ± 5.09	32.16 ± 2.34	6.1 ± 0.39	18.57 ± 0.97	13.32 ± 1.53	1.54 ± 0.14	$3.3^{+2.23}_{-1.42}$	$119.99^{+6.31}_{-6.07}$ ± 15.26	132.0
650	404.73 ± 3.33	32.94 ± 4.99	19.42 ± 1.82	4.96 ± 0.43	12.83 ± 0.83	10.11 ± 1.33	1.25 ± 0.14	$1.93^{+1.88}_{-1.05}$	$83.44^{+5.86}_{-5.65}$ ± 10.46	94.0
700	266.9 ± 2.14	21.33 ± 1.24	12.33 ± 1.47	4.17 ± 0.46	9.27 ± 0.79	6.23 ± 1.05	0.86 ± 0.12	$1.23^{+1.62}_{-0.79}$	$55.41^{+2.88}_{-2.51}$ ± 7.76	71.0
750	180.15 ± 1.4	14.52 ± 0.86	10.07 ± 1.32	3.71 ± 0.53	6.79 ± 0.69	4.57 ± 0.9	0.64 ± 0.09	$0.76^{+1.76}_{-0.63}$	$41.05^{+2.67}_{-2.11}$ ± 6.03	49.0
800	125.24 ± 0.93	12.72 ± 0.94	6.51 ± 1.06	3.37 ± 0.6	5.27 ± 0.5	3.27 ± 0.78	0.5 ± 0.08	$0.76^{+1.76}_{-0.63}$	$32.4^{+2.51}_{-1.9}$ ± 5.44	38.0
850	86.48 ± 0.63	12.41 ± 1.1	5.23 ± 0.94	3.15 ± 0.65	3.41 ± 0.7	2.26 ± 0.64	0.56 ± 0.13	$0.76^{+1.76}_{-0.63}$	$27.79^{+2.55}_{-1.95}$ ± 5.12	28.0
900	60.7 ± 0.43	10.53 ± 1.11	3.75 ± 0.82	2.98 ± 0.69	3.08 ± 0.7	1.99 ± 0.6	0.44 ± 0.12	$0.76^{+1.76}_{-0.63}$	$23.54^{+2.52}_{-1.91}$ ± 4.43	21.0
950	43.79 ± 0.3	8.24 ± 0.92	2.81 ± 0.7	0.66 ± 0.08	2.62 ± 0.69	1.99 ± 0.6	0.31 ± 0.08	$0.76^{+1.76}_{-0.63}$	$17.39^{+2.29}_{-1.61}$ ± 3.5	20.0
1000	31.14 ± 0.21	7.8 ± 0.85	2.03 ± 0.59	0.56 ± 0.07	2.19 ± 0.68	$1.8^{+0.77}_{-0.56}$	0.13 ± 0.03	$0.76^{+1.76}_{-0.63}$	$15.26^{+2.28}_{-1.5}$ ± 3.0	15.0
1050	23.03 ± 0.15	6.87 ± 0.82	$1.58^{+0.72}_{-0.52}$	0.52 ± 0.07	2.14 ± 0.69	$1.41^{+0.7}_{-0.49}$	0.15 ± 0.03	$0.76^{+1.76}_{-0.63}$	$13.43^{+2.29}_{-1.43}$ ± 2.74	14.0
1100	16.69 ± 0.11	6.01 ± 0.78	$1.19^{+0.64}_{-0.44}$	0.47 ± 0.07	1.82 ± 0.67	$1.32^{+0.71}_{-0.49}$	0.15 ± 0.03	$0.76^{+1.76}_{-0.63}$	$11.72^{+2.25}_{-1.38}$ ± 2.33	12.0
1150	12.39 ± 0.08	5.23 ± 0.82	$0.91^{+0.62}_{-0.39}$	0.42 ± 0.07	1.37 ± 0.65	$1.14^{+0.68}_{-0.45}$	0.08 ± 0.02	$0.76^{+1.76}_{-0.63}$	$9.92^{+2.24}_{-1.37}$ ± 1.88	12.0
1200	9.14 ± 0.06	5.04 ± 1.03	$0.73^{+0.58}_{-0.35}$	0.38 ± 0.07	1.26 ± 0.65	$1.14^{+0.68}_{-0.45}$	0.1 ± 0.03	$0.76^{+1.76}_{-0.63}$	$9.4^{+2.32}_{-1.49}$ ± 1.75	10.0
1250	7.08 ± 0.04	4.87 ± 1.02	$0.73^{+0.58}_{-0.35}$	0.37 ± 0.07	1.11 ± 0.65	$1.14^{+0.68}_{-0.45}$	0.1 ± 0.03	$0.76^{+1.76}_{-0.63}$	$9.08^{+2.31}_{-1.48}$ ± 1.64	9.0
1300	5.35 ± 0.03	4.87 ± 1.02	$0.73^{+0.58}_{-0.35}$	0.37 ± 0.07	1.11 ± 0.65	$1.14^{+0.68}_{-0.45}$	0.1 ± 0.03	$0.76^{+1.76}_{-0.63}$	$9.08^{+2.31}_{-1.48}$ ± 1.64	9.0
1350	4.14 ± 0.02	4.87 ± 1.02	$0.73^{+0.58}_{-0.35}$	0.37 ± 0.07	1.11 ± 0.65	$1.14^{+0.68}_{-0.45}$	0.1 ± 0.03	$0.76^{+1.76}_{-0.63}$	$9.08^{+2.31}_{-1.48}$ ± 1.64	9.0
1400	3.14 ± 0.02	4.87 ± 1.02	$0.73^{+0.58}_{-0.35}$	0.37 ± 0.07	1.11 ± 0.65	$1.14^{+0.68}_{-0.45}$	0.1 ± 0.03	$0.76^{+1.76}_{-0.63}$	$9.08^{+2.31}_{-1.48}$ ± 1.64	9.0
1450	2.42 ± 0.01	4.87 ± 1.02	$0.73^{+0.58}_{-0.35}$	0.37 ± 0.07	1.11 ± 0.65	$1.14^{+0.68}_{-0.45}$	0.1 ± 0.03	$0.76^{+1.76}_{-0.63}$	$9.08^{+2.31}_{-1.48}$ ± 1.64	9.0
1500	1.86 ± 0.01	4.87 ± 1.02	$0.73^{+0.58}_{-0.35}$	0.37 ± 0.07	1.11 ± 0.65	$1.14^{+0.68}_{-0.45}$	0.1 ± 0.03	$0.76^{+1.76}_{-0.63}$	$9.08^{+2.31}_{-1.48}$ ± 1.64	9.0
1550	1.4 ± 0.01	4.87 ± 1.02	$0.73^{+0.58}_{-0.35}$	0.37 ± 0.07	1.11 ± 0.65	$1.14^{+0.68}_{-0.45}$	0.1 ± 0.03	$0.76^{+1.76}_{-0.63}$	$9.08^{+2.31}_{-1.48}$ ± 1.64	9.0
1600	1.08 ± 0.01	4.87 ± 1.02	$0.73^{+0.58}_{-0.35}$	0.37 ± 0.07	1.11 ± 0.65	$1.14^{+0.68}_{-0.45}$	0.1 ± 0.03	$0.76^{+1.76}_{-0.63}$	$9.08^{+2.31}_{-1.48}$ ± 1.64	9.0
1650	0.83 ± 0.004	4.87 ± 1.02	$0.73^{+0.58}_{-0.35}$	0.37 ± 0.07	1.11 ± 0.65	$1.14^{+0.68}_{-0.45}$	0.1 ± 0.03	$0.76^{+1.76}_{-0.63}$	$9.08^{+2.31}_{-1.48}$ ± 1.64	9.0
1700	0.64 ± 0.003	4.87 ± 1.02	$0.73^{+0.58}_{-0.35}$	0.37 ± 0.07	1.11 ± 0.65	$1.14^{+0.68}_{-0.45}$	0.1 ± 0.03	$0.76^{+1.76}_{-0.63}$	$9.08^{+2.31}_{-1.48}$ ± 1.64	9.0
1750	0.49 ± 0.002	4.87 ± 1.02	$0.73^{+0.58}_{-0.35}$	0.37 ± 0.07	1.11 ± 0.65	$1.14^{+0.68}_{-0.45}$	0.1 ± 0.03	$0.76^{+1.76}_{-0.63}$	$9.08^{+2.31}_{-1.48}$ ± 1.64	9.0
1800	0.38 ± 0.002	4.87 ± 1.02	$0.73^{+0.58}_{-0.35}$	0.37 ± 0.07	1.11 ± 0.65	$1.14^{+0.68}_{-0.45}$	0.1 ± 0.03	$0.76^{+1.76}_{-0.63}$	$9.08^{+2.31}_{-1.48}$ ± 1.64	9.0
1850	0.29 ± 0.001	4.87 ± 1.02	$0.73^{+0.58}_{-0.35}$	0.37 ± 0.07	1.11 ± 0.65	$1.14^{+0.68}_{-0.45}$	0.1 ± 0.03	$0.76^{+1.76}_{-0.63}$	$9.08^{+2.31}_{-1.48}$ ± 1.64	9.0
1900	0.23 ± 0.001	4.87 ± 1.02	$0.73^{+0.58}_{-0.35}$	0.37 ± 0.07	1.11 ± 0.65	$1.14^{+0.68}_{-0.45}$	0.1 ± 0.03	$0.76^{+1.76}_{-0.63}$	$9.08^{+2.31}_{-1.48}$ ± 1.64	9.0
1950	0.18 ± 0.001	4.87 ± 1.02	$0.73^{+0.58}_{-0.35}$	0.37 ± 0.07	1.11 ± 0.65	$1.14^{+0.68}_{-0.45}$	0.1 ± 0.03	$0.76^{+1.76}_{-0.63}$	$9.08^{+2.31}_{-1.48}$ ± 1.64	9.0
2000	0.14 ± 0.001	4.87 ± 1.02	$0.73^{+0.58}_{-0.35}$	0.37 ± 0.07	1.11 ± 0.65	$1.14^{+0.68}_{-0.45}$	0.1 ± 0.03	$0.76^{+1.76}_{-0.63}$	$9.08^{+2.31}_{-1.48}$ ± 1.64	9.0

Event filters applied

- *HBHE noise filter: available in MiniAOD*
- *HBHE isolated noise filter: available in MiniAOD*
- *CSC beam halo filter: The "globalTightHalo2016" version of the filter is used; available in MiniAOD*
- *Good primary vertex filter: The event must have a well-defined good quality primary vertex; available in MiniAOD*
- *Bad EE supercrystal filter: Events with unusually high energies in four ECAL endcap supercrystals are removed; available in MiniAOD*
- *Bad resolution track filter: Rejects events containing a high-p_T charged hadron with unusually high p_T resolution; re-run on top of MiniAOD*
- *Bad muon track filter: Rejects events containing high-p_T muons with either (1) unusually high p_T resolution; (2) high χ^2/ndf without muon system hits; or (3) no muon subtrack having good p_T resolution; re-run on top of MiniAOD*

Loose Jet ID

- *Neutral hadron energy fraction less than 0.99*
- *Neutral electromagnetic energy fraction less than 0.99*
- *At least two constituents*
- *Charged hadron energy fraction greater than 0*
- *Charged multiplicity greater than 0*
- *Charged electromagnetic energy fraction less than 0.99*

8TeV Limits

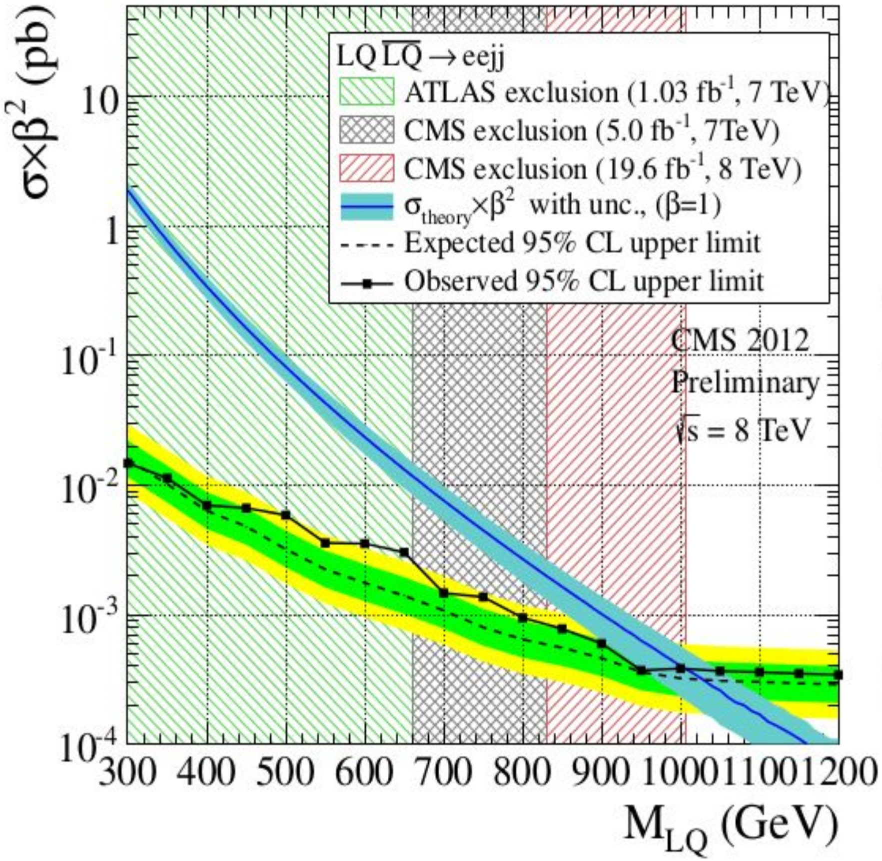

$\sigma\times\beta^2$ (pb)
LQ $\overline{LQ}$ → eejj
ATLAS exclusion (1.03 fb^{-1}, 7 TeV)
CMS exclusion (5.0 fb^{-1}, 7TeV)
CMS exclusion (19.6 fb^{-1}, 8 TeV)
$\sigma_{theory}\times\beta^2$ with unc., (β=1)
Expected 95% CL upper limit
Observed 95% CL upper limit
CMS 2012
Preliminary
$\sqrt{s}$ = 8 TeV
M_{LQ} (GeV)

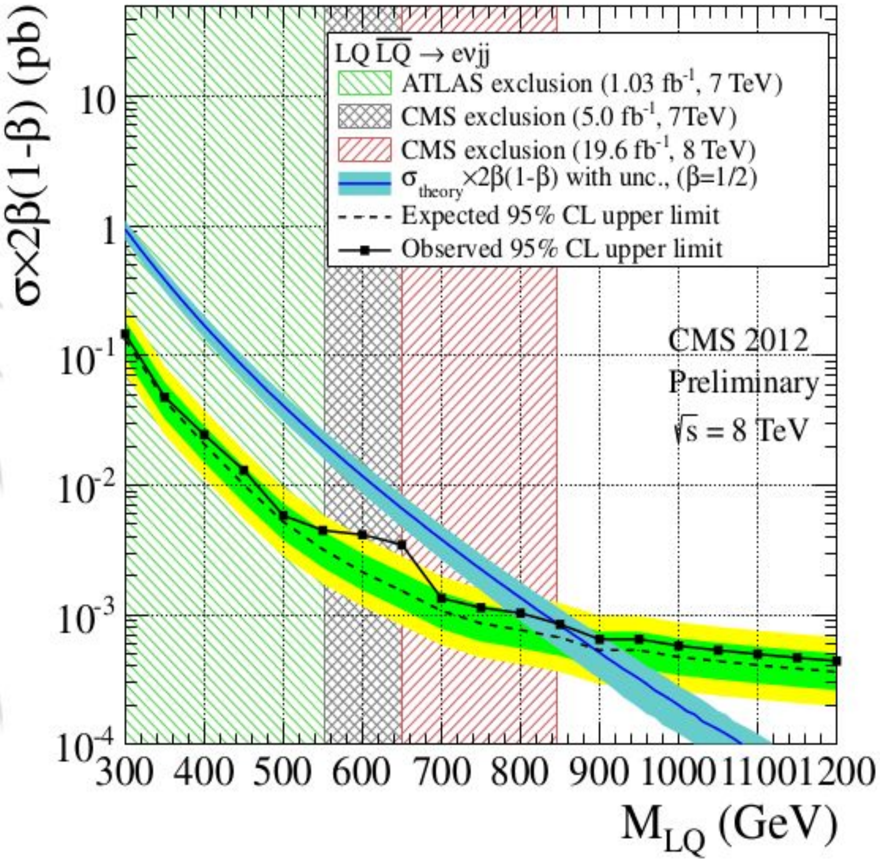

$\sigma\times2\beta(1-\beta)$ (pb)
LQ $\overline{LQ}$ → eνjj
ATLAS exclusion (1.03 fb^{-1}, 7 TeV)
CMS exclusion (5.0 fb^{-1}, 7TeV)
CMS exclusion (19.6 fb^{-1}, 8 TeV)
$\sigma_{theory}\times2\beta(1-\beta)$ with unc., (β=1/2)
Expected 95% CL upper limit
Observed 95% CL upper limit
CMS 2012
Preliminary
$\sqrt{s}$ = 8 TeV
M_{LQ} (GeV)